

High-momentum components in the nuclear symmetry energy

- Isospin dependence of the NN-interaction and Symmetry energy
- Momentum distributions and NN-correlations.
- Single particle spectral functions .
- Tensor contribution to the symmetry energy.
- High momentum components in the nuclear symmetry energy.

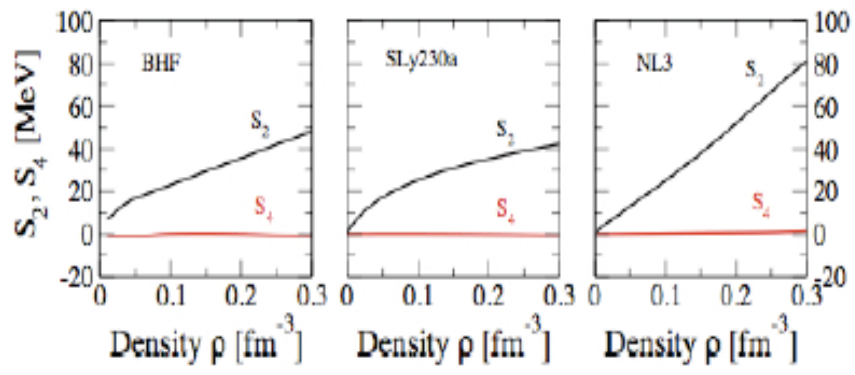
NN-interactions act differently in symmetric nuclear matter than in neutron matter. A “measure” of this isospin dependence is provided by the symmetry energy.

Charge symmetry of nuclear forces \rightarrow Only even powers

Charge symmetry \rightarrow expansion of $(E/A)_{ANM}$ on even powers of isospin asymmetry $\beta = (\rho_n - \rho_p) / (\rho_n + \rho_p)$

$$\frac{E}{A}(\rho, \beta) = E_{SNM}(\rho) + S_2(\rho)\beta^2 + S_4(\rho)\beta^4 + O(\beta^6)$$

$$E_{SNM}(\rho) = \frac{E}{A}(\rho, \beta = 0), \quad S_2(\rho) = \frac{1}{2} \left. \frac{\partial^2 E/A}{\partial \beta^2} \right|_{\beta=0}, \quad S_4(\rho) = \frac{1}{24} \left. \frac{\partial^4 E/A}{\partial \beta^4} \right|_{\beta=0}$$



In good approximation:

$$S_2(\rho) \sim \frac{E}{A}(\rho, \beta = 1) - \frac{E}{A}(\rho, \beta = 0)$$

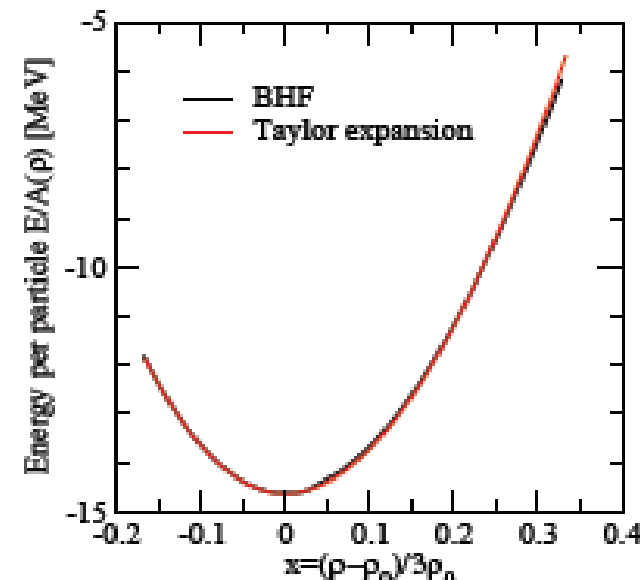
Taylor expansion of the energy per particle of symmetric nuclear matter around the saturation density.

$$E_{SNM}(\rho) = E_0 + \frac{K_0}{2!} \left(\frac{\rho - \rho_0}{3\rho_0} \right)^2 + \frac{Q_0}{3!} \left(\frac{\rho - \rho_0}{3\rho_0} \right)^3 + \mathcal{O}(4)$$

$$E_0 = E_{SNM}(\rho = \rho_0) \sim -16 \text{ MeV}$$

$$K_0 = 9\rho_0^2 \left. \frac{\partial^2 E_{SNM}(\rho)}{\partial \rho^2} \right|_{\rho=\rho_0} \sim 200 \text{ to } 300 \text{ MeV}$$

$$Q_0 = 27\rho_0^3 \left. \frac{\partial^3 E_{SNM}(\rho)}{\partial \rho^3} \right|_{\rho=\rho_0} \sim -500 \text{ to } +300 \text{ MeV}$$

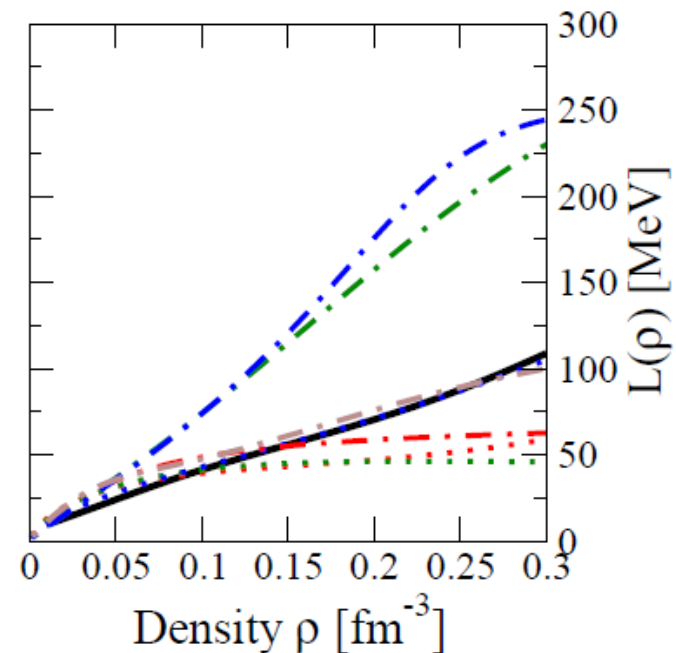
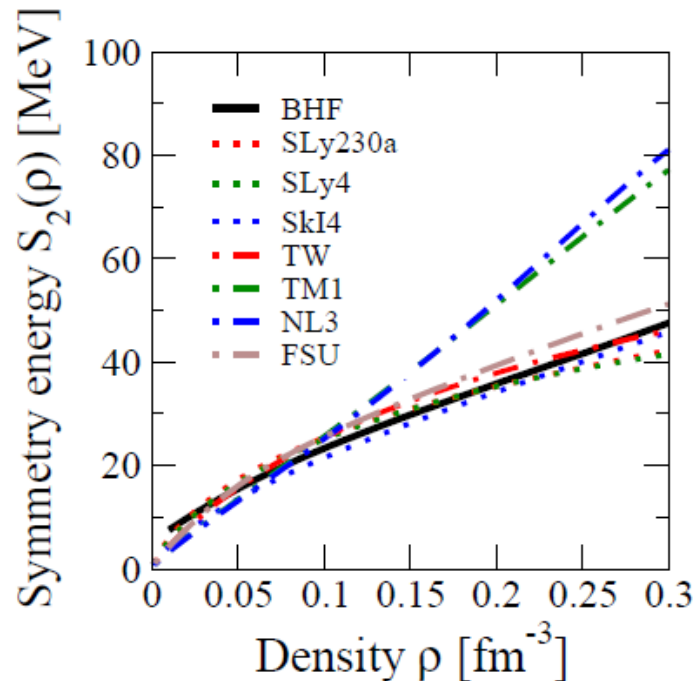


The behavior of the symmetry energy around saturation can be also characterized in terms of a few bulk parameters.

$$S_2(\rho) = E_{sym} + L \left(\frac{\rho - \rho_0}{3\rho_0} \right) + \frac{K_{sym}}{2!} \left(\frac{\rho - \rho_0}{3\rho_0} \right)^2 + \frac{Q_{sym}}{3!} \left(\frac{\rho - \rho_0}{3\rho_0} \right)^3 + \mathcal{O}(4)$$

$$E_{sym} \sim 30 - 32 \text{ MeV} \quad L = 3\rho_0 \left. \frac{\partial S_2(\rho)}{\partial \rho} \right|_{\rho=\rho_0}$$

$$K_{sym} = 9\rho_0^2 \left. \frac{\partial^2 S_2(\rho)}{\partial \rho^2} \right|_{\rho=\rho_0} \quad Q_{sym} = 27\rho_0^3 \left. \frac{\partial^3 S_2(\rho)}{\partial \rho^3} \right|_{\rho=\rho_0}$$



Combining the precedent expansions, one can predict the existence of a saturation density, i.e., a zero pressure condition, for a given asymmetry and rewrite the energy per particle of asymmetric matter around the new saturation density

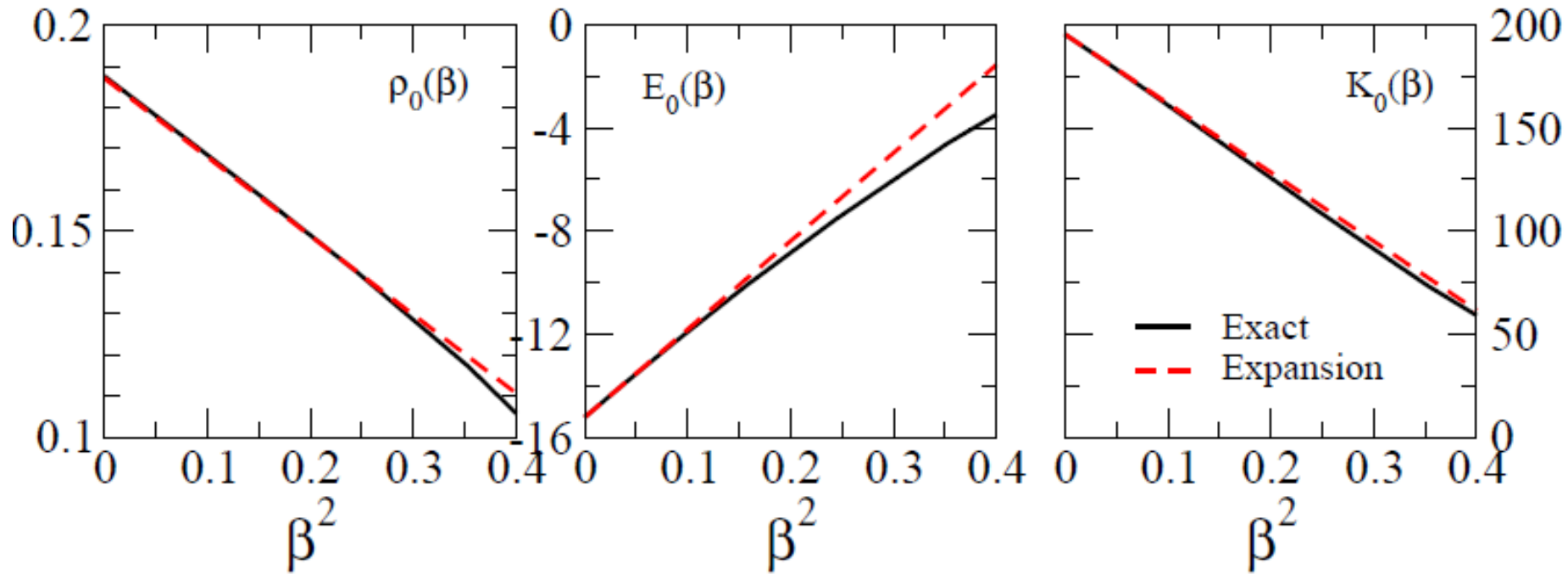
$$\frac{E}{A}(\rho, \beta) = E_0(\beta) + \frac{K_0(\beta)}{2!} \left(\frac{\rho - \rho_0(\beta)}{3\rho_0(\beta)} \right)^2 + \frac{Q_0(\beta)}{3!} \left(\frac{\rho - \rho_0(\beta)}{3\rho_0(\beta)} \right)^3 + \mathcal{O}(4)$$

$$\rho_0(\beta) = \rho_0 \left(1 - 3 \frac{L}{K_0} \beta^2 \right) + \mathcal{O}(4)$$

$$E_0(\beta) = E_0 + E_{sym} \beta^2 + \mathcal{O}(4)$$

$$K_0(\beta) = K_0 + \underbrace{\left(K_{sym} - 6L - \frac{Q_0}{K_0} L \right)}_{K_\tau} \beta^2 + \mathcal{O}(4)$$

$$Q_0(\beta) = Q_0 + \left(Q_{sym} - 9L \frac{Q_0}{K_0} \right) \beta^2 + \mathcal{O}(4)$$



Isospin asymmetry dependence of the saturation density, energy per particle and incompressibility coefficient at the saturation point of asymmetric nuclear matter.

Solid lines show the results of the exact BHF calculations whereas dashed lines indicates the results of the previous expansion.

All quantities in MeV, except the density

Model	ρ_0	E_0	K_0	Q_0	E_{sym}	L	K_{sym}	Q_{sym}	K_τ	Ref.
BHF (with TBFa)	0.187	-15.23	195.5	-280.9	34.3	66.5	-31.3	-112.8	-334.7	
BHF (with TBFb)	0.176	-14.62	185.9	-224.9	33.6	66.9	-23.4	-162.8	-343.8	
BHF (without TBF)	0.240	-17.30	213.6	-225.1	35.8	63.1	-27.8	-159.8	-339.6	
SLy4	0.159	-15.97	229.8	-362.9	31.8	45.3	-119.8	520.8	-320.4	[8]
SLy10	0.155	-15.90	229.7	-358.3	32.1	39.2	-142.4	590.9	-316.7	[9]
SLy230a	0.160	-15.98	229.9	-364.2	31.8	43.9	-98.4	602.8	-292.7	[10]
SkI4	0.162	-16.15	250.3	-335.7	29.6	59.9	-43.4	358.8	-322.5	[37]
SkI5	0.156	-15.84	255.6	-301.7	36.4	128.9	159.8	11.2	-461.6	[37]
SkI6	0.159	-15.88	248.2	-326.7	34.4	82.1	-0.9	332.3	-385.8	[38]

BHF approximation of ANM

Energy per particle

$$\blacksquare \frac{E}{A}(\rho, \beta) = \frac{1}{A} \sum_{\tau} \sum_{k \leq k_F} \left(\frac{\hbar^2 k^2}{2m_{\tau}} + \frac{1}{2} \text{Re}[U_{\tau}(\vec{k})] \right)$$



Infinite summation of **two-hole line** diagrams

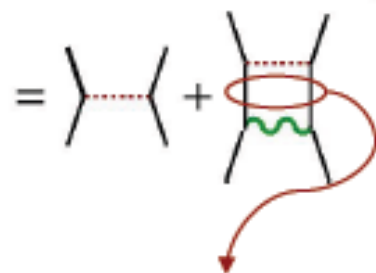
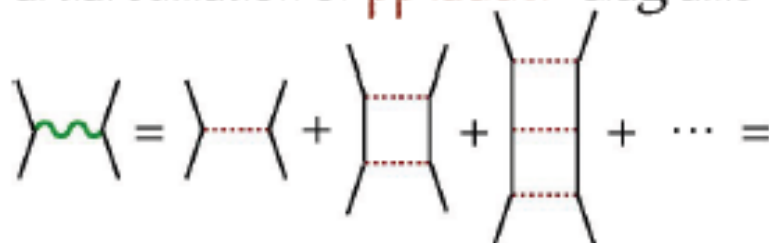
Bethe-Goldstone Equation

$$\blacksquare G(\omega) = V + V \frac{Q}{\omega - E - E' + i\eta} G(\omega)$$

$$\blacksquare E_{\tau}(k) = \frac{\hbar^2 k^2}{2m_{\tau}} + \text{Re}[U_{\tau}(k)]$$

$$\blacksquare U_{\tau}(k) = \sum_{\tau'} \sum_{k' \leq k_{F, \tau'}} \langle \vec{k} \vec{k}' | G(\omega = E_{\tau}(k) + E_{\tau'}(k')) | \vec{k} \vec{k}' \rangle_A$$

Partial summation of **pp ladder** diagrams



✓ Pauli blocking

✓ Nucleon dressing

Neutron matter with the simplest Skyrme force

$$V = \sum_{i < j} (t_0 + \frac{1}{6} t_3 \rho^\gamma) \delta(\vec{r}_i - \vec{r}_j)$$

The two-body matrix element:

$$\langle \vec{k}_1 m_{s1}, \vec{k}_2 m_{s2} | v_{12} | \vec{k}_1 m_{s1}, \vec{k}_2 m_{s2} - \vec{k}_2 m_{s2}, \vec{k}_1 m_{s1} \rangle = \frac{1}{\Omega} (t_0 + \frac{t_3}{6} \rho^\gamma) (1 - \delta_{m_{s1} m_{s2}})$$

Summing up all the matrix elements as we did for nuclear matter we get

$$\frac{\langle \phi_{FS} | V | \phi_{FS} \rangle}{N} = \frac{1}{2} \rho (t_0 + \frac{t_3}{6} \rho^\gamma) \frac{1}{2}$$

The total energy per particle:

$$e_{PNM}(\rho) = \frac{\hbar^2}{2m} \frac{3}{5} (3\pi^2)^{2/3} \rho^{2/3} + \frac{1}{2} \rho (t_0 + \frac{t_3}{6} \rho^\gamma) \frac{1}{2}$$

The energy per particle for nuclear matter

$$e_{SNM}(\rho) = \frac{\hbar^2}{2m} \frac{3}{5} \left(\frac{3\pi^2}{2}\right)^{2/3} \rho^{2/3} + \frac{1}{2}\rho(t_0 + \frac{t_3}{6}\rho^\gamma) \frac{3}{4}$$

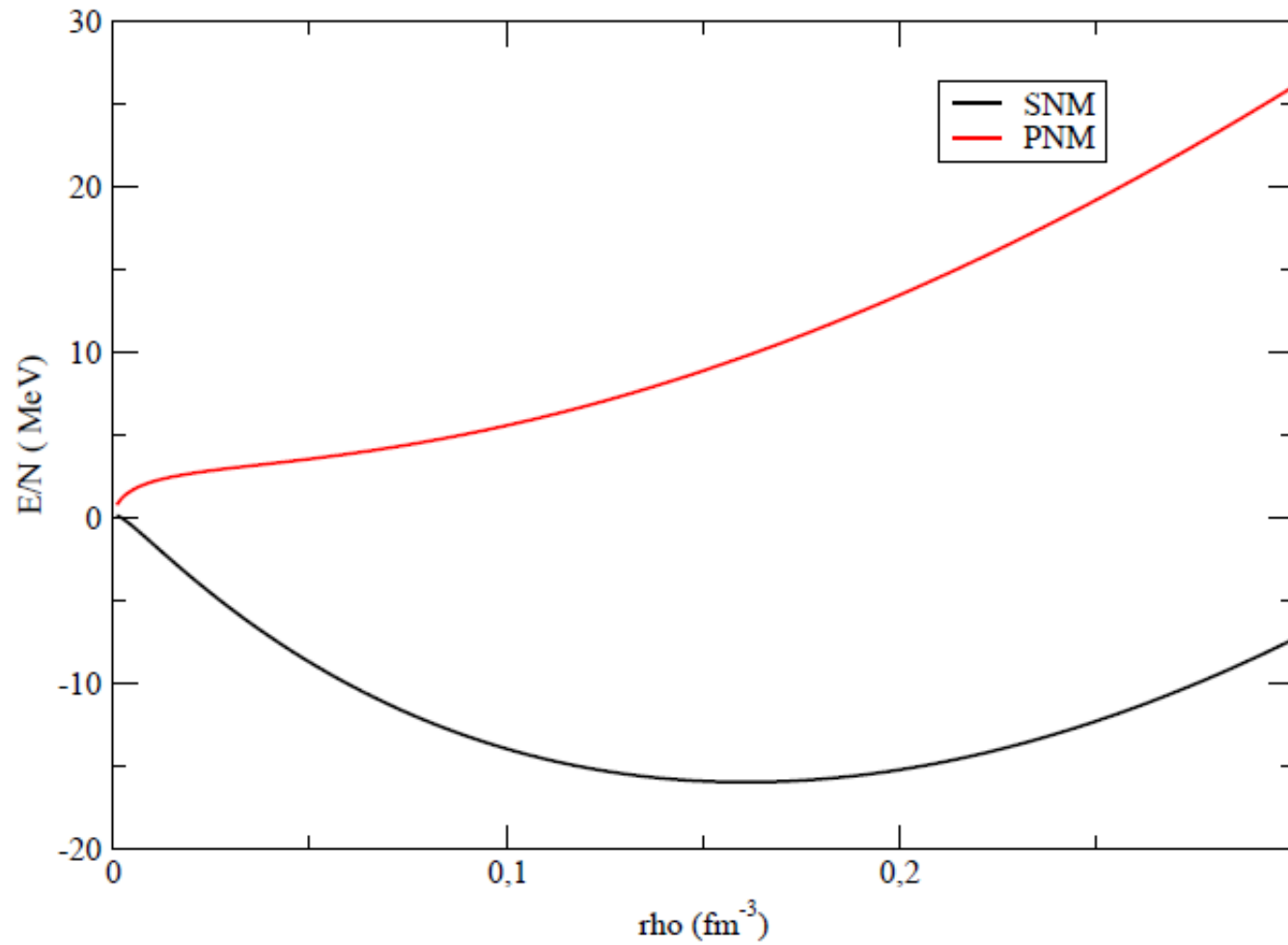
Then the symmetry energy as a function of the density calculated as the difference between the energy per particle of pure neutrón matter and symmetric nuclear matter is given by

$$e_{sym} = \frac{\hbar^2}{2m} \frac{3}{5} (3\pi^2)^{2/3} \rho^{2/3} \left[1 - \left(\frac{1}{2}\right)^{2/3}\right] - \frac{1}{2}\rho(t_0 + \frac{t_3}{6}\rho^\gamma) \frac{1}{4}$$

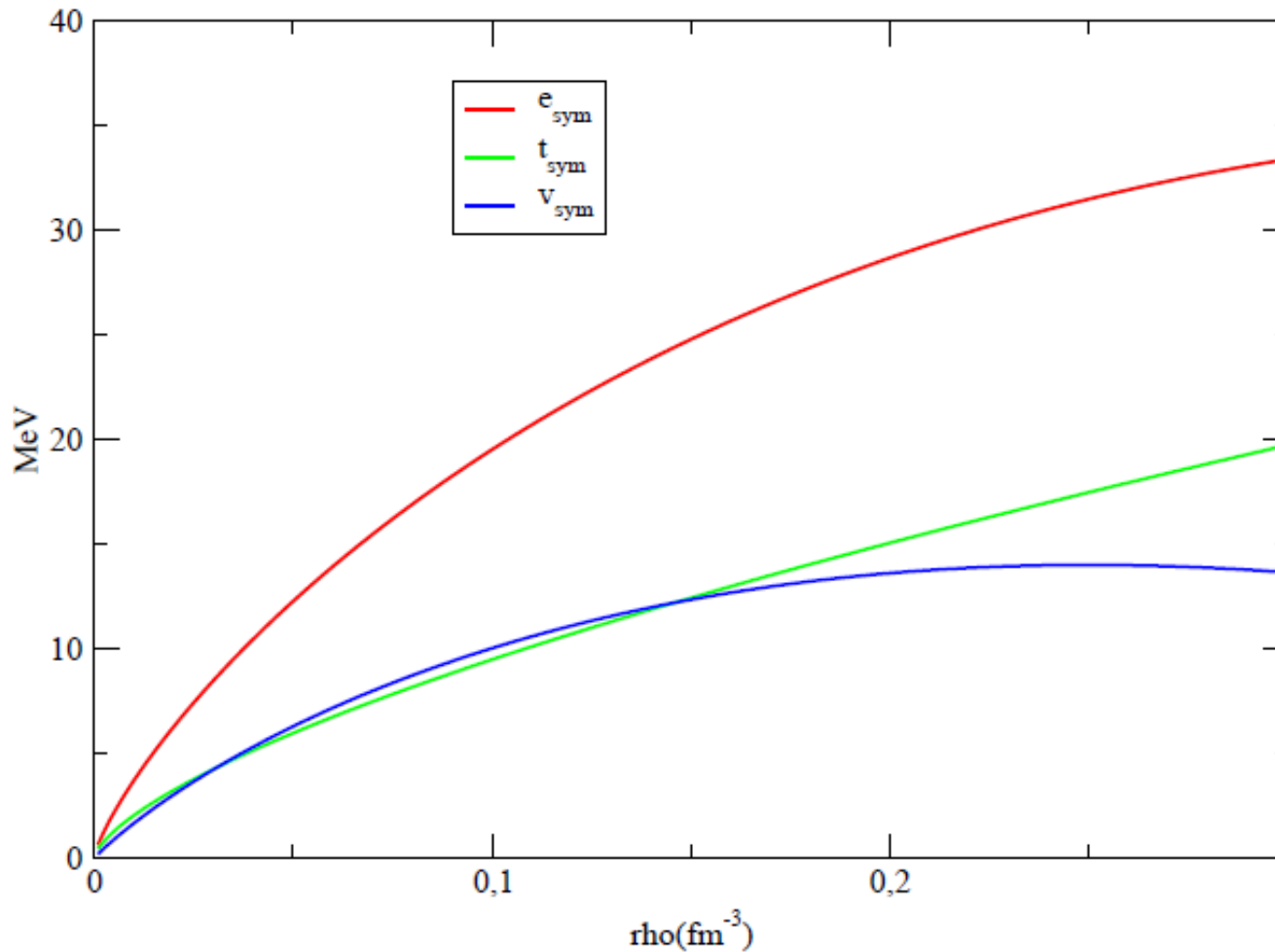
$\rho = 0.16 \text{ fm}^{-3}$ we have $e_{sym} = 25.7 \text{ MeV}$

with $t_{sym} = 12.9 \text{ MeV}$ and $v_{sym} = 12.7 \text{ MeV}$

$$L = 3\rho_0 \frac{de_{sym}}{d\rho} = 40.8 \text{ MeV}$$



Energy of neutron and nuclear matter



Symmetry energy decomposed in the kinetic and potential Contributions.

$$e_{sym} = 25.7 \text{ MeV at } \rho = 0.16 \text{ fm}^{-3}$$

By construction, mean field calculations, with effective interactions, do not give access to the high-momentum components. Their associated $n(k)$ are just uncorrelated step-functions.

BHF provides the energy correction to the non-interacting system (free Fermi sea) but do not provide the separate contributions of the kinetic energy and potential energy in the correlated many-body state.

We have observed the isospin dependence, either of the effective interactions or of the realistic interactions looking at the results (mean field and BHF) for nuclear and neutron matter.

A new insight of the importance of correlations can be provided by analyzing the kinetic and potential energy contribution to the symmetry energy and the contribution of the difference components of the potential

Can we do that in the BHF framework?

How high-momentum components produced by NN-correlations affect the symmetry energy?

If correlations are measured by the departure of $n(k)$ from the step function. Which system is more correlated nuclear matter or neutron matter ? How are the the momentum distributions of asymmetric nuclear matter?

Which components of the interaction are responsible for the symmetry energy?

Correlation effects on $n(p)$ for nuclear matter.

Units. Energy in Mev and lengths in fm

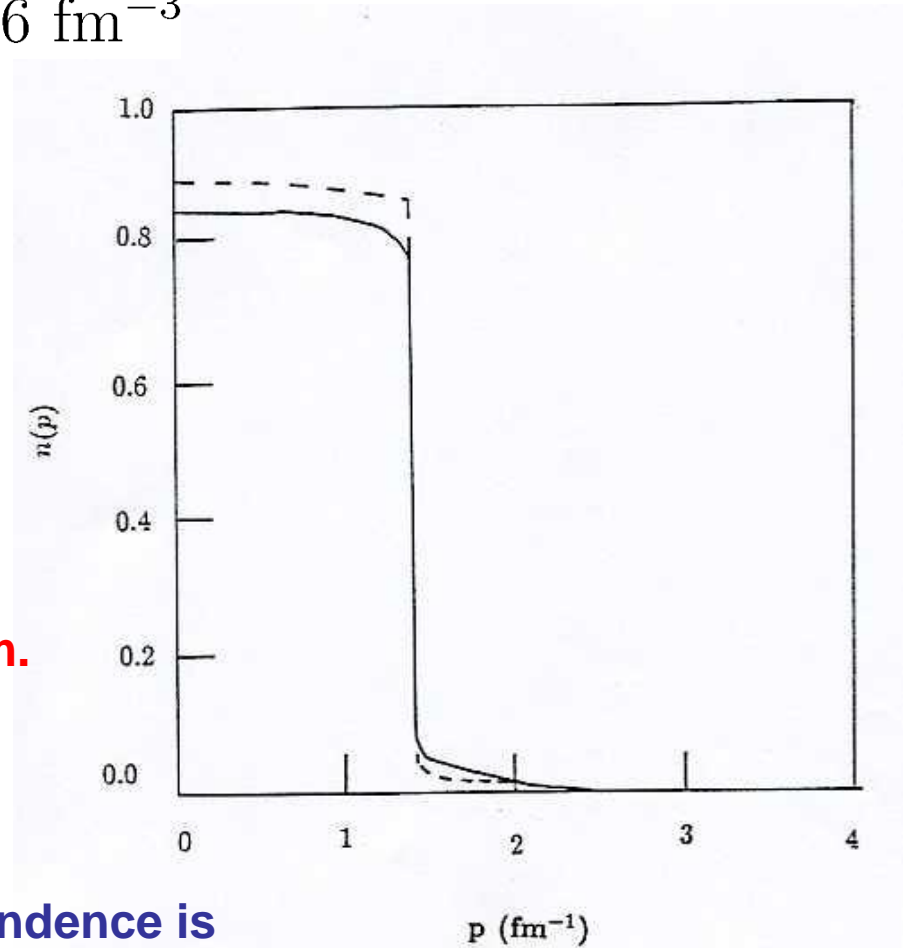
Depletion rather constant below the Fermi momentum. Around 15 per cent

$$k_F = 1.36 \text{ fm}^{-1} \quad \rho = 0.16 \text{ fm}^{-3}$$

$$Z_{k_F} \sim 0.7$$

$$\langle T \rangle \sim 43 \text{ MeV}$$

$$\langle T \rangle_{FFG} \sim 23 \text{ MeV}$$



Depletion below the Fermi momentum.
High momentum components in the
correlated wave function.

We will explore how the isospin dependence is
reflected in the correlated nature of $n(k)$.

The Hellmann-Feynman theorem in conjunction with BHF can be used to estimate the “true” kinetic energy.

Hellmann-Feynman theorem:

Consider a Hamiltonian depending on a parameter

$$\frac{dE_\lambda}{d\lambda} = \frac{\langle \psi_\lambda | \frac{d\hat{H}_\lambda}{d\lambda} | \psi_\lambda \rangle}{\langle \psi_\lambda | \psi_\lambda \rangle}$$

The nuclear Hamiltonian can be decomposed in a kinetic and a potential Energy pieces:

$$\hat{H} = \hat{T} + \hat{V}$$

Defining a λ depending Hamiltonian:

$$\hat{H}_\lambda = \hat{T} + \lambda \hat{V}$$

The expectation value of the potential energy

$$\langle \hat{V} \rangle = \frac{\langle \psi | \hat{V} | \psi \rangle}{\langle \psi | \psi \rangle} = \left(\frac{dE_\lambda}{d\lambda} \right) \Big|_{\lambda=1}$$

For Av18+Urbana IX three-body force at saturation density

$$\rho_0 = 0.187 \text{ fm}^{-3}$$

	E_{NM}	E_{SM}	E_{sym}	L
$\langle T \rangle$	53.321	54.294	-0.973	14.896
$\langle V \rangle$	-34.251	-69.524	35.273	51.604
Total	19.070	-15.230	34.300	66.500

The major contribution to both E_{sym} and L is due to the potential energy

The kinetic contribution to E_{sym} is very small and negative

In contrast, the FFG approach to the symmetry energy is ~ 14.4 MeV. The contribution of the kinetic energy to L is smaller than the FFG which amounts ~ 29.2 MeV

$$E_{\text{FFG}}(\text{SM}) = 24.53 \text{ MeV}, \quad T(\text{SM}) - E_{\text{FFG}}(\text{SM}) = 29.76 \text{ MeV}$$

$$E_{\text{FFG}}(\text{NM}) = 38.94 \text{ MeV}, \quad T(\text{NM}) - E_{\text{FFG}}(\text{NM}) = 14.38 \text{ MeV}$$

(S, T)	E_{NM}	E_{SM}	E_{sym}	L
(0, 0)	0	5.600	-5.600	-21.457
(0, 1)	-29.889	-23.064	-6.825	-17.950
(1, 0)	0	-49.836	49.836	90.561
(1, 1)	-4.362	-2.224	-2.138	0.450

TABLE III: Spin (S) and isospin (T) channel decomposition of the potential part of E_{NM} , E_{SM} , E_{sym} and L . Units are given in MeV.

Largest contributions from S=1, T=0 channel which is not present in neutron matter.

Similar T=1 channel contributions to E_{NM} and to E_{SM} which almost cancel out in E_{sym}

TABLE I. Deuteron D -state probability P_D , quadrupole moment Q_d (in fm²), total binding energy, kinetic and potential energy, and their decomposition in partial waves, for different potentials. All energies are given in MeV.

Force	P_D (%)	Q_d	E	T	V	T_S	T_D	V_S	V_D	$2V_{SD}$
V_{18}	5.78	0.27	-2.24	19.86	-22.10	11.30	8.56	-3.95	0.77	-18.91
V'_8	5.78	0.27	-2.24	19.86	-22.10	11.30	8.56	-3.95	0.77	-18.91
V'_6	5.33	0.27	-2.24	18.70	-20.94	11.38	7.32	-4.68	1.38	-17.64
V'_4	0.00	0.00	-2.24	11.41	-13.65	11.41	0.0	-13.65	0.0	0.0
\tilde{V}_6	4.64	0.30	-1.46	14.96	-16.42	9.10	5.86	-3.43	1.14	-14.14

$$T_S = \langle {}^3S_1 | T | {}^3S_1 \rangle$$

$$T_D = \langle {}^3D_1 | T | {}^3D_1 \rangle$$

$$V_S = \langle {}^3S_1 | V | {}^3S_1 \rangle$$

$$V_D = \langle {}^3D_1 | V | {}^3D_1 \rangle$$

$$V_{SD} = \langle {}^3S_1 | V | {}^3D_1 \rangle$$

The binding in the deuteron is also the result of a strong cancelation between the potential and the kinetic energy.

Partial wave	E_{NM}	E_{SM}	E_{sym}	L					
1S_0	-23.070	-19.660	-3.410	-3.459	-				
3S_1	0	-45.810	45.810	71.855	3H_4	0.033	0.040	-0.007	0.232
1P_1	0	4.904	-4.904	-18.601	3H_5	0.225	-0.033	0.258	0.968
3P_0	-5.321	-4.029	-1.292	-1.898	3H_6	0.043	0.034	0.009	0.144
3P_1	16.110	10.720	5.390	21.949	1I_6	-0.082	0.023	-0.105	-0.591
3P_2	-16.000	-9.334	-6.666	-21.168	3I_5	0	-0.029	0.029	0.342
1D_2	-5.956	-3.201	-2.755	-11.033	3I_6	0	0.067	-0.067	-0.819
3D_1	0	0.981	-0.981	-3.739	3I_7	0	-0.021	0.021	0.239
3D_2	0	-3.982	3.982	16.601	1J_7	0	-0.027	0.027	0.385
3D_3	0	-0.798	0.798	4.895	3J_6	0.044	0.020	0.024	0.283
1F_3	0	0.694	-0.694	-3.348	3J_7	-0.062	-0.060	-0.002	-0.313
3F_2	-0.695	-0.229	-0.466	-1.799	3J_8	0.036	0.014	0.022	0.242
3F_3	2.000	0.821	1.179	4.883	1K_8	0.031	0.021	0.010	0.169
3F_4	-0.796	-0.194	-0.602	-3.239	3K_7	0	-0.011	0.011	0.138
1G_4	-0.812	-0.247	-0.565	-3.036	3K_8	0	0.038	-0.038	-0.491
3G_3	0	-0.001	0.001	0.441	3L_8	0.021	0.006	0.015	0.166
3G_4	0	-0.213	0.213	0.449					
3G_5	0	-0.057	0.057	0.650					
1H_5	0	0.029	-0.029	0.107					

3S_1 wave gives the larger contribution to the symmetry energy and L

Large cancellations between the other partial waves.

	E_{NM}	E_{SM}	E_{sym}	L
3S_1	0	-45.810	45.810	71.855
3D_1	0	-0.981	0.981	-3.739
$\Sigma_{\text{rest up to } J=8}$	-34.251	-22.733	-11.518	-16.512

✓ Main contribution
from 3S_1 - 3D_1 p.w. (not
present in NM)

	E_{NM}	E_{SM}	E_{sym}	L
$\langle V_1 \rangle$	-31.212	-32.710	1.498	-5.580
$\langle V_{\vec{\tau}_i \cdot \vec{\tau}_j} \rangle$	-4.957	3.997	-8.954	-20.383
$\langle V_{\vec{\sigma}_i \cdot \vec{\sigma}_j} \rangle$	-0.319	-0.382	0.063	2.392
$\langle V_{(\vec{\sigma}_i \cdot \vec{\sigma}_j)(\vec{\tau}_i \cdot \vec{\tau}_j)} \rangle$	-5.724	-11.388	5.664	2.521
$\langle V_{S_{ij}} \rangle$	-0.792	1.912	-2.704	-4.998
$\langle V_{S_{ij}(\vec{\tau}_i \cdot \vec{\tau}_j)} \rangle$	-4.989	-37.592	32.603	47.095
$\langle V_{\vec{L} \cdot \vec{S}} \rangle$	-7.538	-1.754	-5.784	-12.251
$\langle V_{\vec{L} \cdot \vec{S}(\vec{\tau}_i \cdot \vec{\tau}_j)} \rangle$	-2.671	-6.539	3.868	3.969
$\langle V_{L^2} \rangle$	11.850	13.610	-1.760	1.521
$\langle V_{L^2(\vec{\tau}_i \cdot \vec{\tau}_j)} \rangle$	-2.788	0.270	-3.058	-14.262
$\langle V_{L^2(\vec{\sigma}_i \cdot \vec{\sigma}_j)} \rangle$	1.265	1.383	-0.118	1.405
$\langle V_{L^2(\vec{\sigma}_i \cdot \vec{\sigma}_j)(\vec{\tau}_i \cdot \vec{\tau}_j)} \rangle$	0.051	0.008	0.043	-0.341
$\langle V_{(\vec{L} \cdot \vec{S})^2} \rangle$	4.194	5.682	-1.488	-0.327
$\langle V_{(\vec{L} \cdot \vec{S})^2(\vec{\tau}_i \cdot \vec{\tau}_j)} \rangle$	5.169	-6.190	11.359	31.368
$\langle V_{T_{ij}} \rangle$	0.003	0.039	-0.036	-0.022
$\langle V_{(\vec{\sigma}_i \cdot \vec{\sigma}_j)T_{ij}} \rangle$	-0.017	-0.106	0.089	0.042
$\langle V_{S_{ij}T_{ij}} \rangle$	0.004	0.079	-0.075	-0.124
$\langle V_{(\tau_{z_i} + \tau_{z_j})} \rangle$	-0.084	-0.001	-0.083	-0.331
$\langle U_1 \rangle$	2.985	3.251	-0.266	-0.630
$\langle U_{(\vec{\sigma}_i \cdot \vec{\sigma}_j)(\vec{\tau}_i \cdot \vec{\tau}_j)} \rangle$	2.254	3.999	-1.745	-7.228
$\langle U_{S_{ij}(\vec{\tau}_i \cdot \vec{\tau}_j)} \rangle$	-0.935	-7.092	6.157	27.768

Separate contributions from the various components of Av18 and the two-body reduced Urbana force. All energies in MeV

The largest contribution is from the tensor component

Up to now, we have considered only an integrated property of $n(k)$, i.e., the kinetic energy. Now we want to look in more detail on $n(k)$. To this end we will use the single-particle propagator.

The Single particle propagator a good tool to study single particle properties

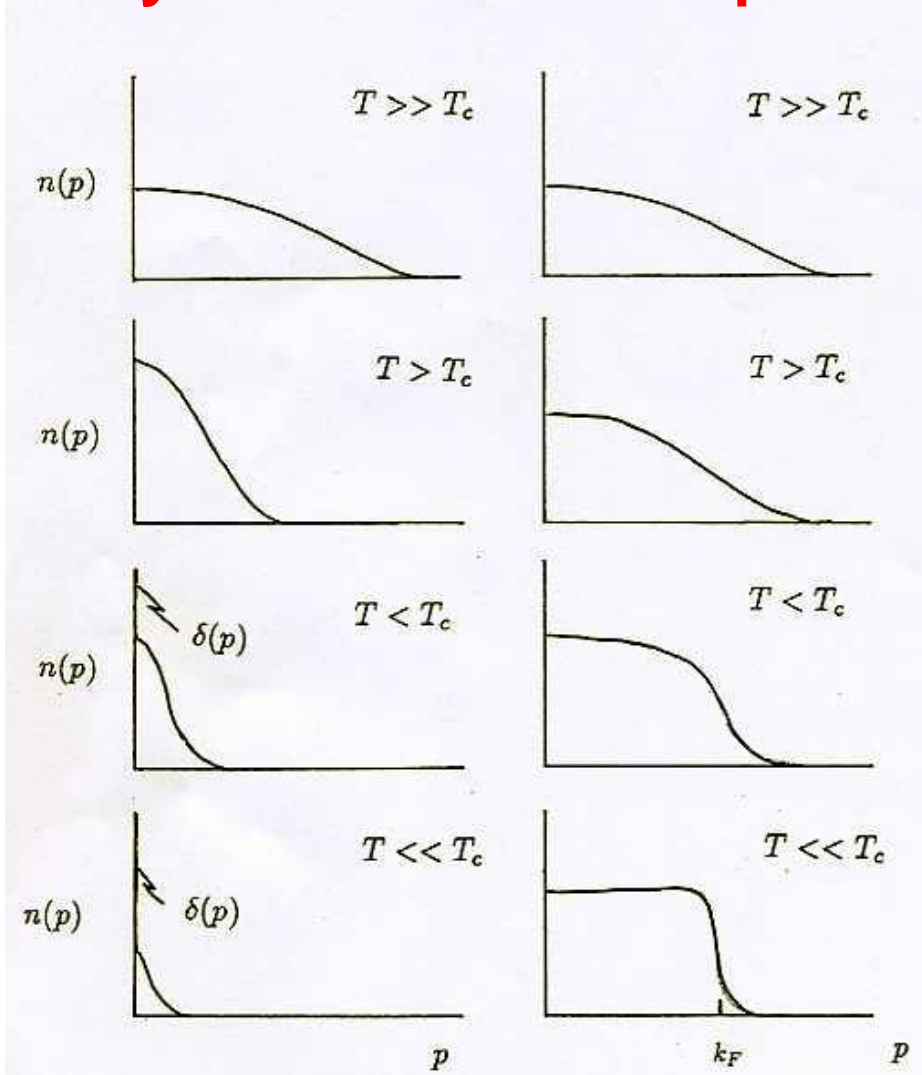
Not necessary to know all the details of the system (the full many-body wave function) but just what happens when we add or remove a particle to the system.

It gives access to all single particle properties as :

- momentum distributions
- self-energy (Optical potential)
- effective masses
- spectral functions

Also permits to calculate the expectation value of a very special two-body operator: the Hamiltonian in the ground state.

Typical behavior of $n(k)$ as a function of temperature for the ideal Bose and Fermi gases. $n(k)$ is affected by statistics and temperature.



The effects of quantum statistics become dominant below a characteristic temperature T_c .

Macroscopic occupation of the zero momentum state for Bose systems.

Discontinuity of $n(k)$ at the Fermi surface at $T=0$.

Typical behaviour of the momentum distribution and the one-body density matrix in the ground state for interacting Bose and Fermi systems

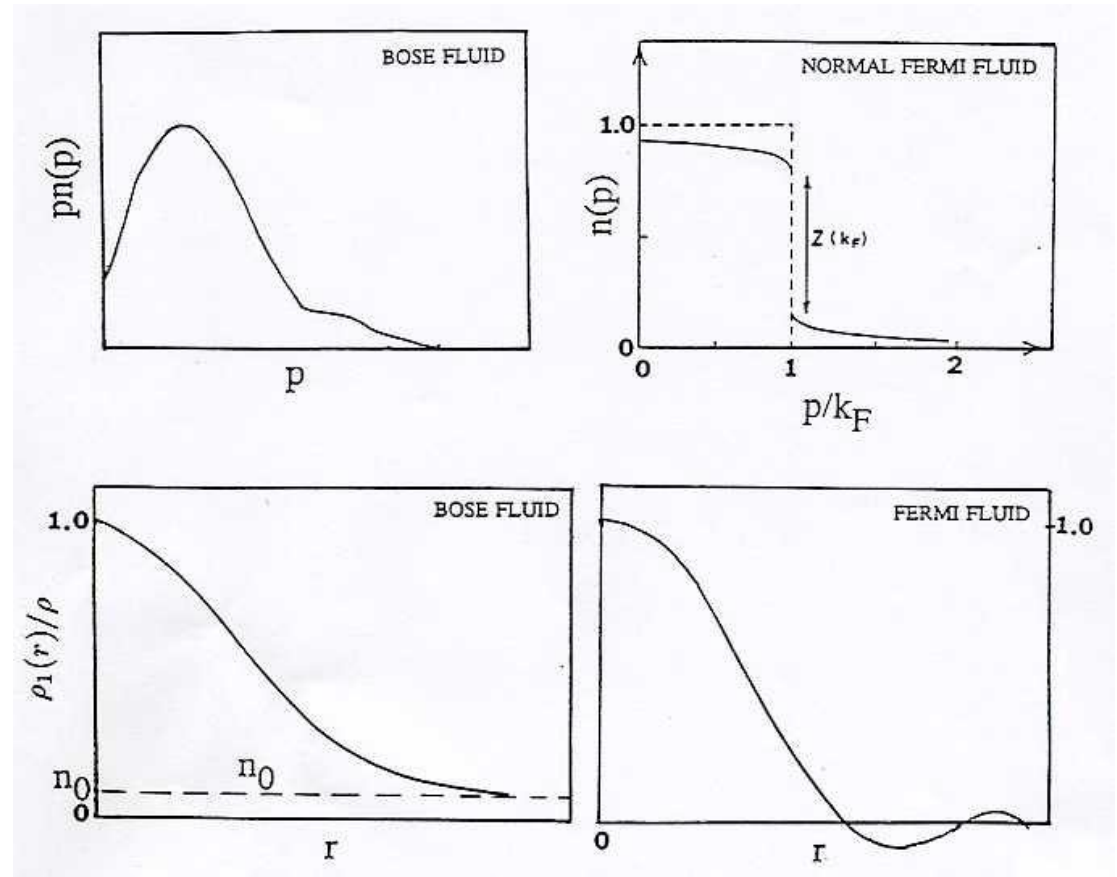
$$\rho_1(\vec{r}_1, \vec{r}'_1) = N \int d^3r_2 \dots d^3r_N \Psi^*(\vec{r}_1, \vec{r}_2, \dots, \vec{r}_N) \Psi(\vec{r}'_1, \vec{r}_2, \dots, \vec{r}_N)$$

$$n(p) = \langle \Psi | a_{\vec{p}}^\dagger a_{\vec{p}} | \Psi \rangle \quad n(p) = \nu^{-1} \int \rho_1(r) e^{i\vec{p}\vec{r}} d^3r$$

$$n(p) = N n_0 \delta_{\vec{p}0} + n'(p)$$

$$n'(p \rightarrow 0) \sim n_0 \frac{mc}{2p}$$

$$n_0 = \lim_{r \rightarrow \infty} \rho_1(r) / \rho$$



Liquid ^3He is a very correlated Fermi liquid.

Large depletion

Units : Energy (K) and length (Å)

$$k_F = 0.789 \text{Å}^{-1}$$

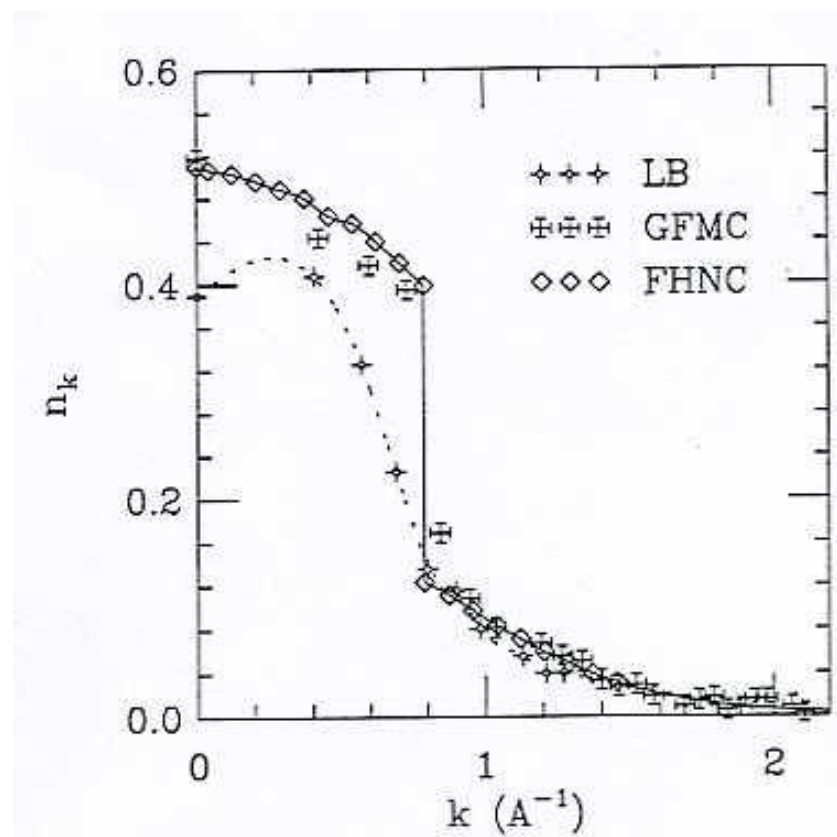
$$E_F \sim 3K$$

$$E_k \sim 12K$$

$$E_B = -2.5K$$

$$Z_{k_F} = 0.275$$

$$(1 - n(0)) \sim 0.5$$



n(p) for nuclear matter.

Units. Energy in Mev and lengths in fm

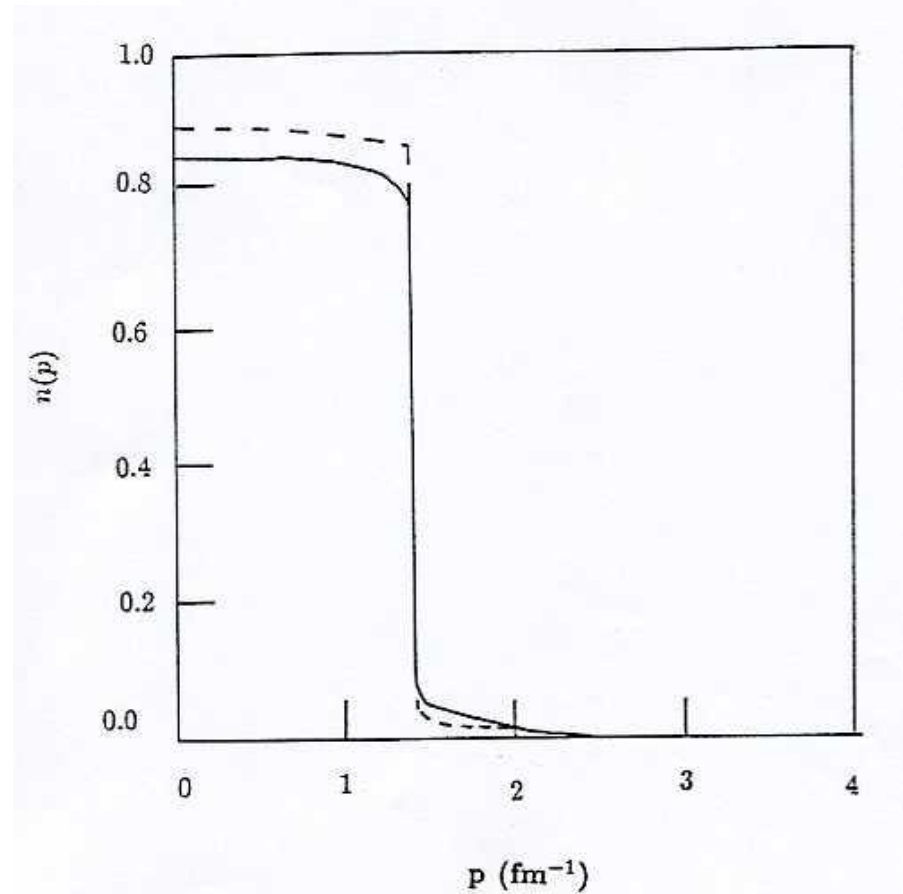
Depletion rather constant below the Fermi momentum. Around 15 per cent

$$k_F = 1.36 \text{ fm}^{-1} \quad \rho = 0.16 \text{ fm}^{-3}$$

$$Z_{k_F} \sim 0.7$$

$$\langle T \rangle \sim 43 \text{ MeV}$$

$$\langle T \rangle_{FFG} \sim 23 \text{ MeV}$$



Lehmann representation + Spectral functions

FT+ closure => Lehmann representation

$$g(k, \omega) = \frac{1}{2\pi} \int_{-\infty}^{\infty} d\omega' \frac{A^>(k, \omega')}{\omega - \omega' + i\eta} + \frac{1}{2\pi} \int_{-\infty}^{\infty} d\omega' \frac{A^<(k, \omega')}{\omega - \omega' - i\eta}$$

$$A^<(k, \omega) = 2\pi \sum_{n,m} \frac{e^{-\beta(E_m - \mu N_m)}}{Z} |\langle \Psi_n | a_{\mathbf{k}} | \Psi_m \rangle|^2 \delta(\omega - (E_m - E_n))$$

$$A^>(k, \omega) = 2\pi \sum_{m,n} \frac{e^{-\beta(E_m - \mu N_m)}}{Z} |\langle \Psi_n | a_{\mathbf{k}}^\dagger | \Psi_m \rangle|^2 \delta(\omega - (E_n - E_m))$$

The summation runs over all energy eigenstates and all particle number eigenstates

The spectral function

$$A(k, \omega) = A^<(k, \omega) + A^>(k, \omega)$$

with

$$A^>(k, \omega) = e^{\beta(\omega - \mu)} A^<(k, \omega)$$

therefore

$$A^<(k, \omega) = A(k, \omega) f(\omega)$$

where

$$f(\omega) = \left\{ e^{\beta(\omega - \mu)} + 1 \right\}^{-1}$$

Is the Fermi function

and

$$A^>(k, \omega) = A(k, \omega)(1 - f(\omega))$$

Momentum distribution

T=0 MeV

$$n(k, T = 0) = \frac{1}{2\pi} \int_{-\infty}^{\epsilon_F} A_h(k, \omega) d\omega$$

Finite T

$$n(k, T) = \frac{1}{2\pi} \int_{-\infty}^{\infty} A^<(k, \omega) d\omega = \frac{1}{2\pi} \int_{-\infty}^{\infty} A(k, \omega) f(\omega) d\omega$$

How to calculate the energy

Koltun sum-rule

$$\frac{E}{A} = \frac{\text{deg}}{\rho} \sum_{\tau} \int \frac{d^3k}{(2\pi)^3} \int_{-\infty}^{\infty} \frac{d\omega}{2\pi} \frac{1}{2} \left(\frac{k^2}{2m} + \omega \right) A_{\tau}(k, \omega) f_{\tau}(\omega)$$

$$A_{\tau}(k, \omega) = \delta(\omega - \epsilon_{\tau}^{BHF}(k))$$

In the BHF $\epsilon_{\tau}^{BHF}(k)$ is the BHF quasi-particle energy

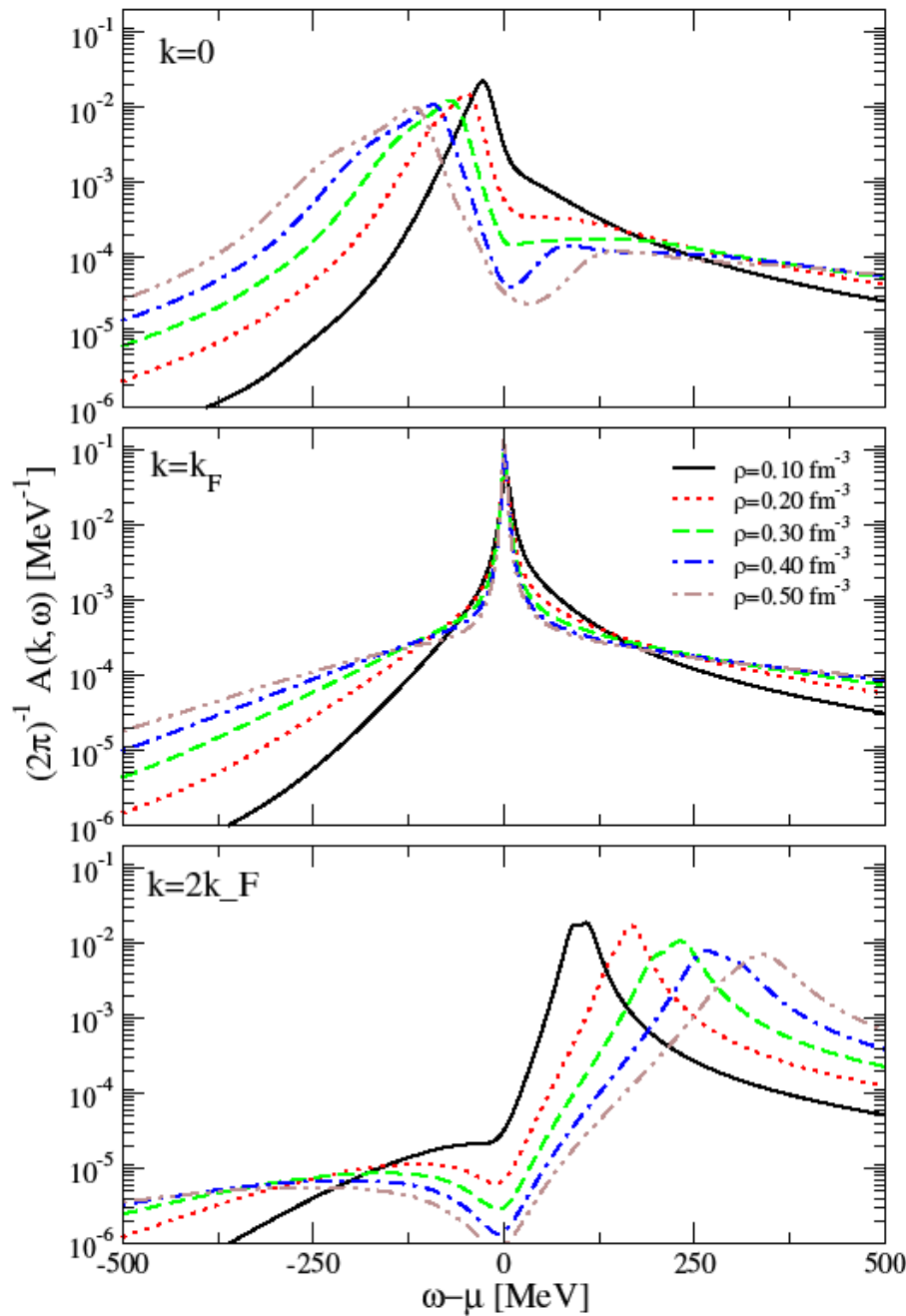
Does not include propagation of holes

The momentum distribution is obtained by convoluting the spectral function with a Fermi Dirac factor.

$$n(k) = \int \frac{d\omega}{2\pi} \mathcal{A}(k, \omega) f(\omega)$$

Calculations are performed at finite T to avoid pairing instabilities.
NO THREE-BODY forces are included.

Symmetric Nuclear Matter, $T=10$ MeV

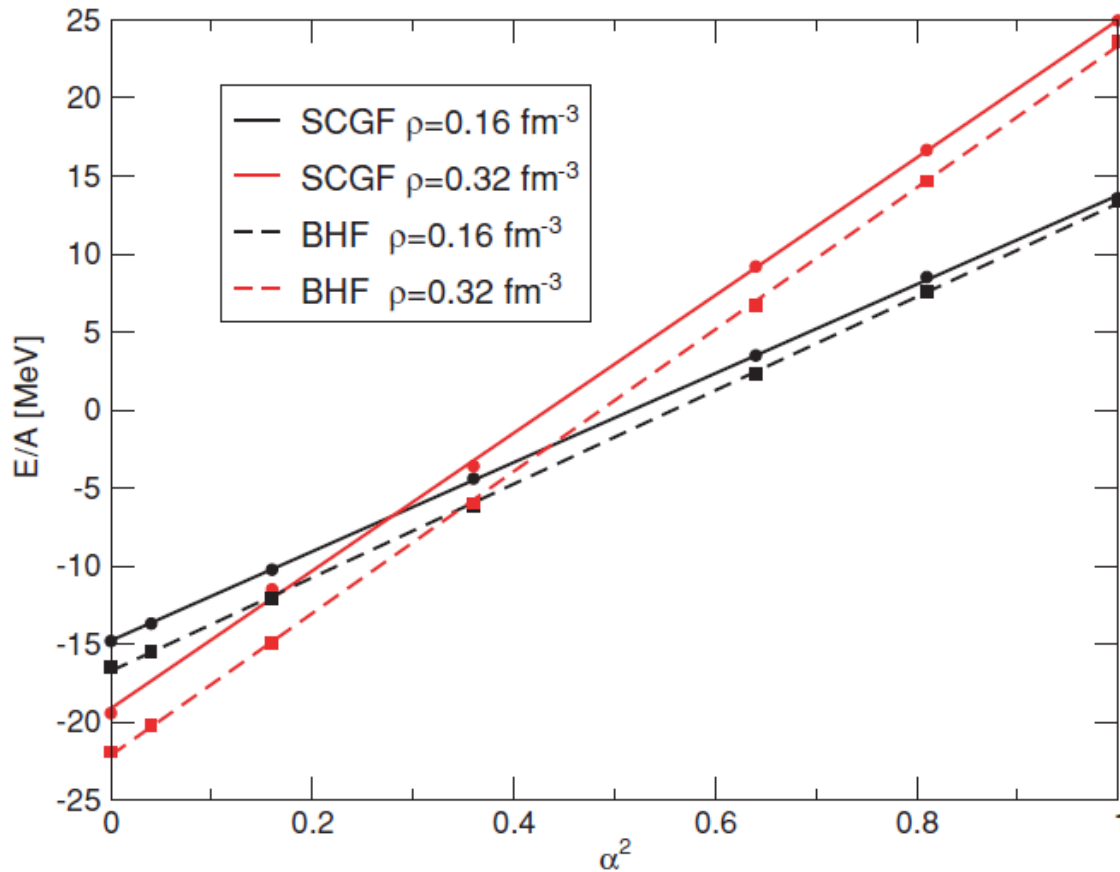


Tails extend to the high energy range.

Quasi-particle peak shifting with density.

Peaks broaden with density.

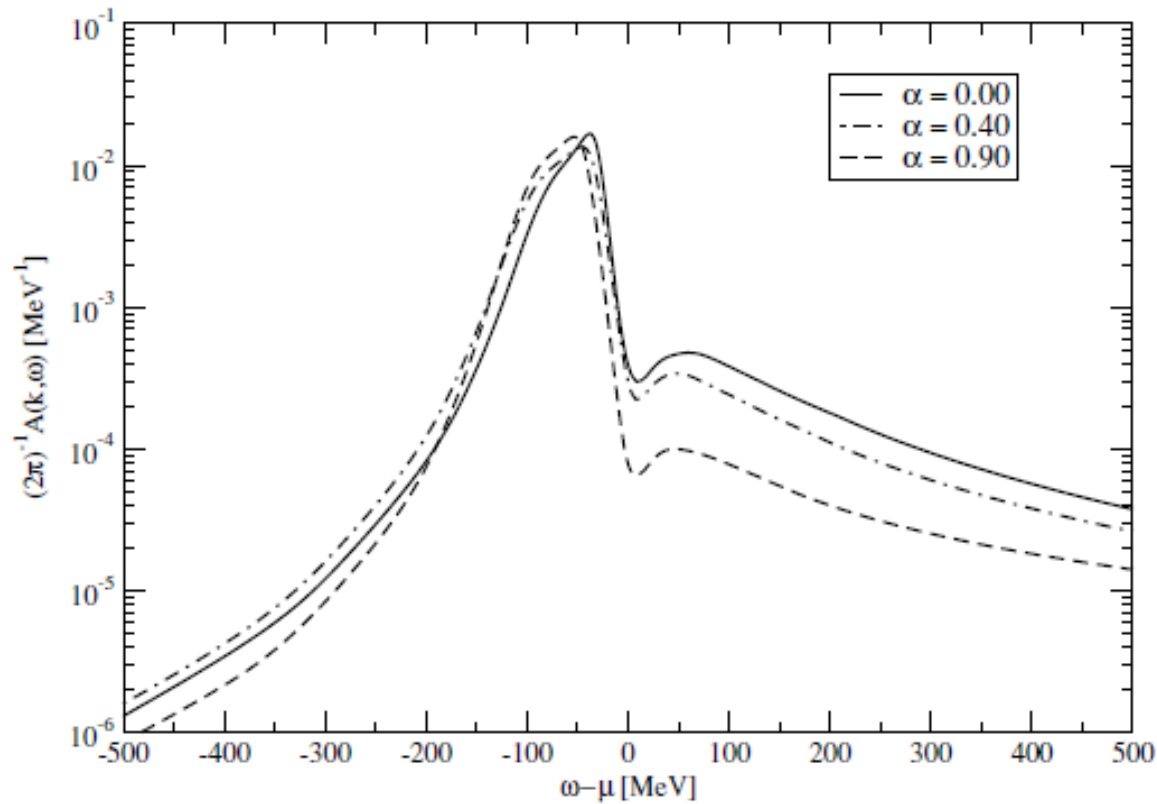
$$T = 5 \text{ MeV}$$



Dependence of the energy per nucleon as a function of the asymmetry square

Linear behavior! Justifies quadratic expansion both for BHF and SCGF.

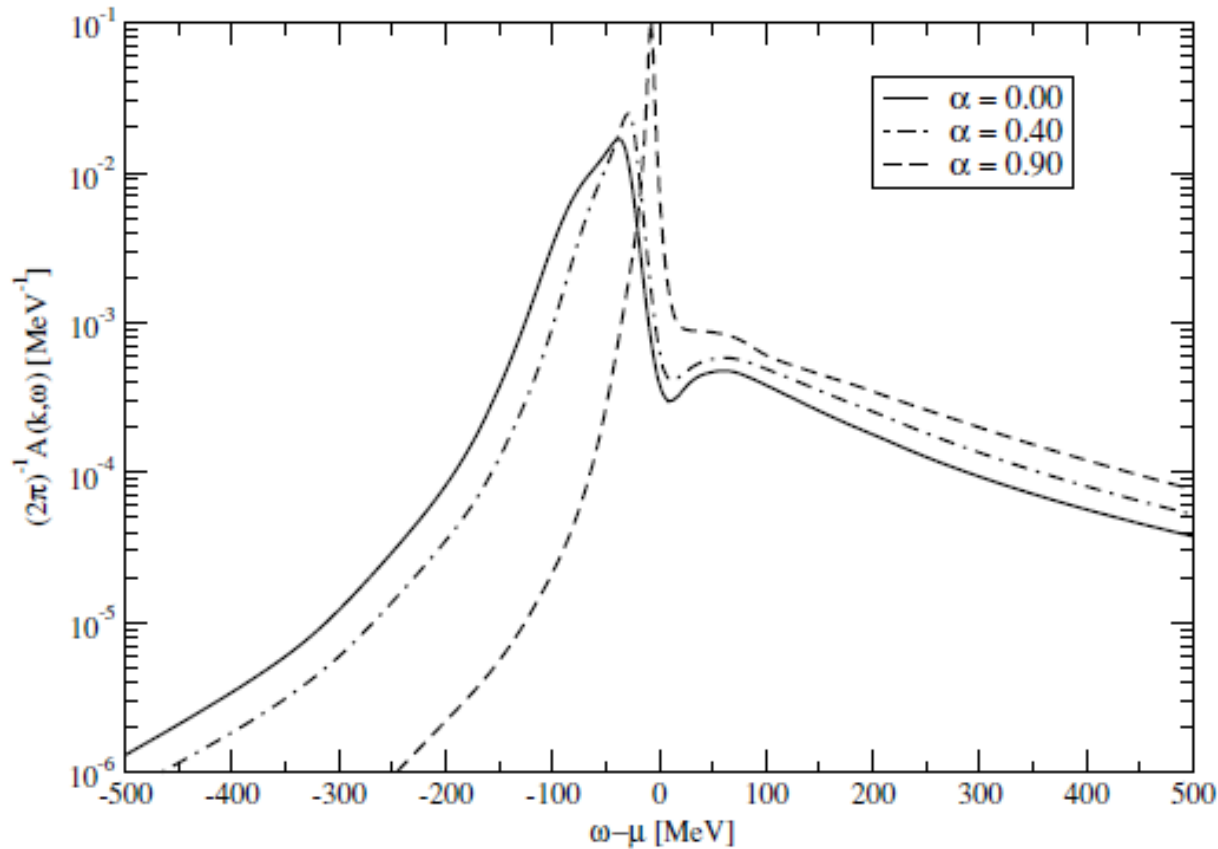
Repulsive effects of the propagation of holes. Smaller for neutron matter than for nuclear matter.



$$\rho = 0.16 \text{fm}^{-3}$$

$$T = 5 \text{ MeV}$$

K=0 MeV, neutron spectral function for different asymmetries. For CDBONN.
The tail of the spectral function at high-energy gets lower. Indicating a decrease of the tensor correlations when the asymmetry increases and the neutrons see less protons.



$$\rho = 0.16 \text{ fm}^{-3}$$

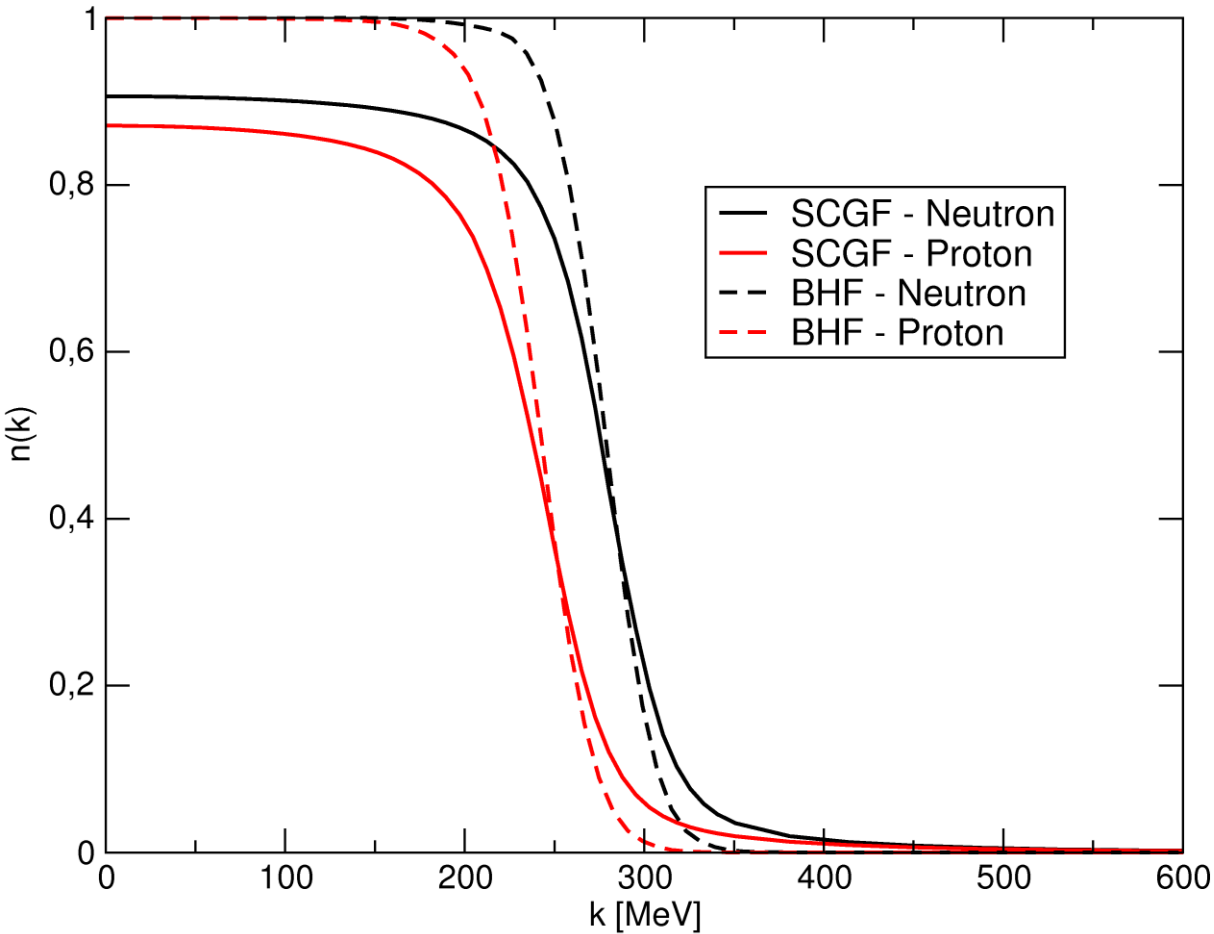
$$T = 5 \text{ MeV}$$

$$k = 0 \text{ MeV}$$

As the asymmetry increases, the Fermi momentum for protons gets closer to zero and therefore the spectral functions gets narrower. However, the high energy tails increase due to the tensor and short Range correlations. The protons see many neutrons.

Proton and neutron momentum distributions $\rho=0.16 \text{ fm}^{-3}$

CDBONN



✓ The BHF $n(k)$ do not contain correlation effects and very similar to a normal thermal Fermi distribution.

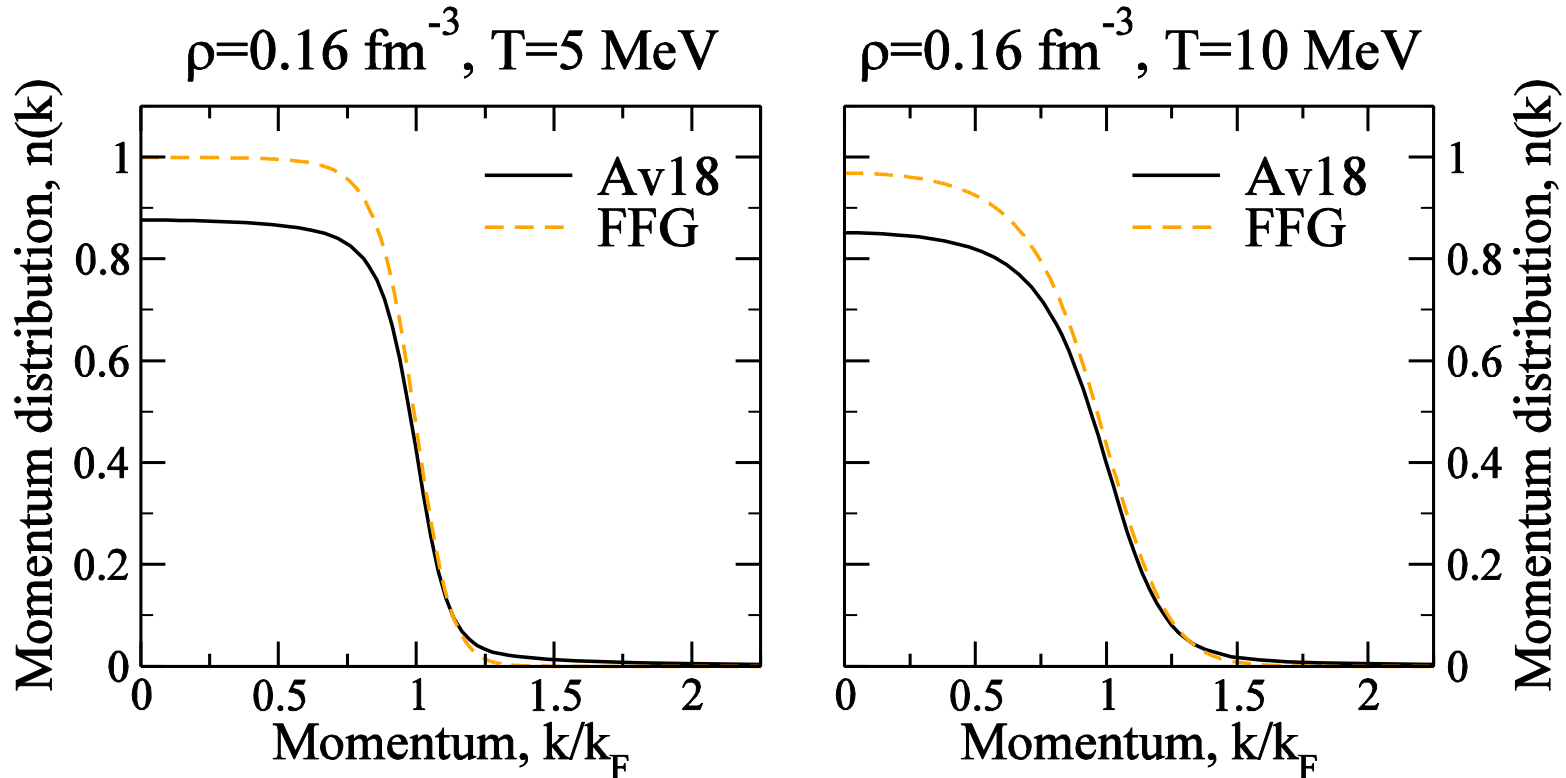
✓ The SCGF $n(k)$ contain thermal and correlation effects.

✓ Depletion at low momenta and larger occupation than the BHF $n(k)$ at larger momenta.

✓ The proton depletion is larger than the neutron depletion.

Momentum distributions for symmetric nuclear matter

At $T=5$ MeV, for FFG $k < k_F$, 86 per cent of the particles! and 73 per cent at $T=10$ MeV. In the correlated case, at $T=5$ MeV for $k < k_F$, 75 per cent and 66 per cent at $T=10$ MeV.

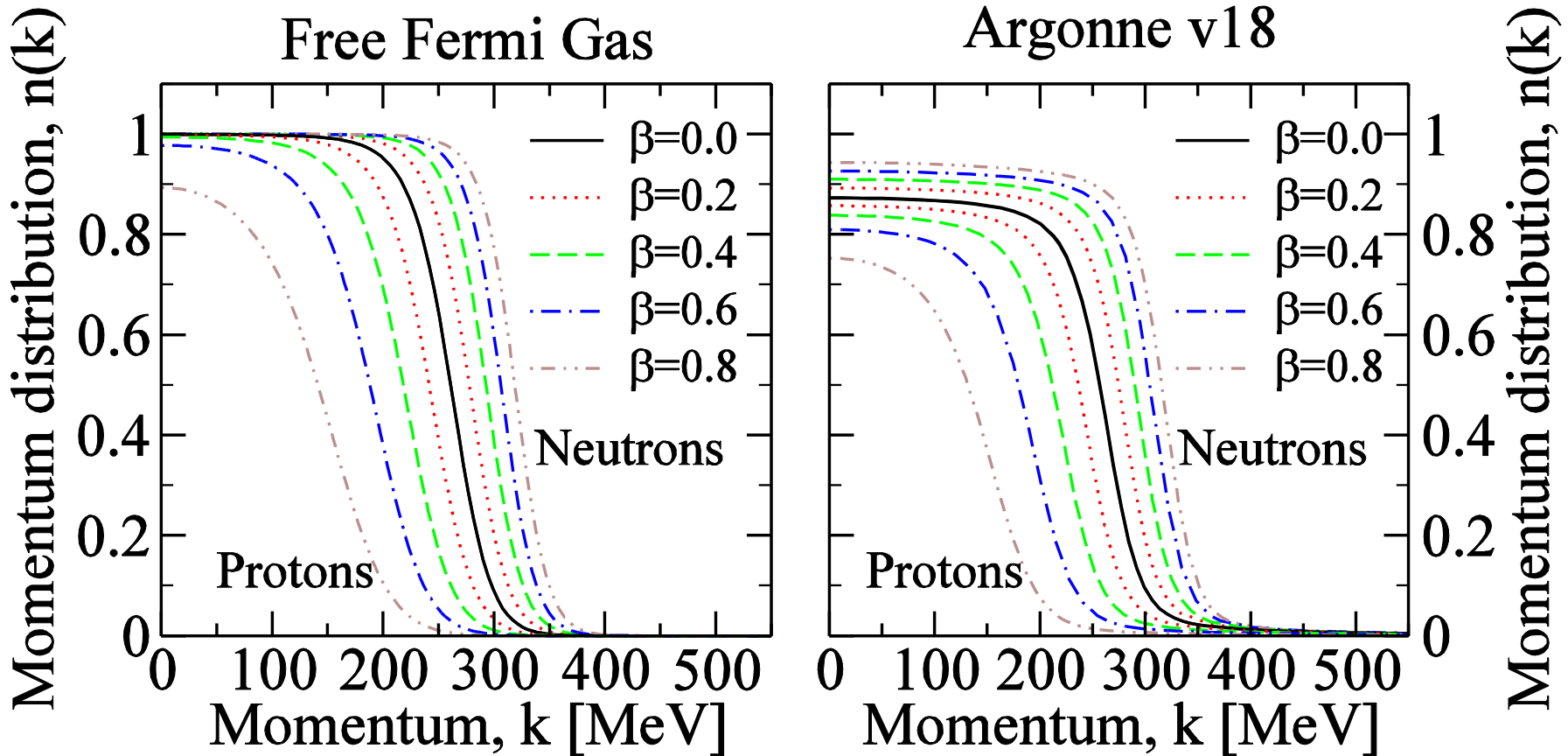


At low T ($T=5$ MeV), thermal effects affect only the Fermi surface.
At large T , they produce also a depletion. The total depletion (around 15 per cent) can be considered the sum of thermal depletion (3 per cent) and the depletion associated to dynamic correlations.

Neutron and proton momentum distributions for different asymmetries

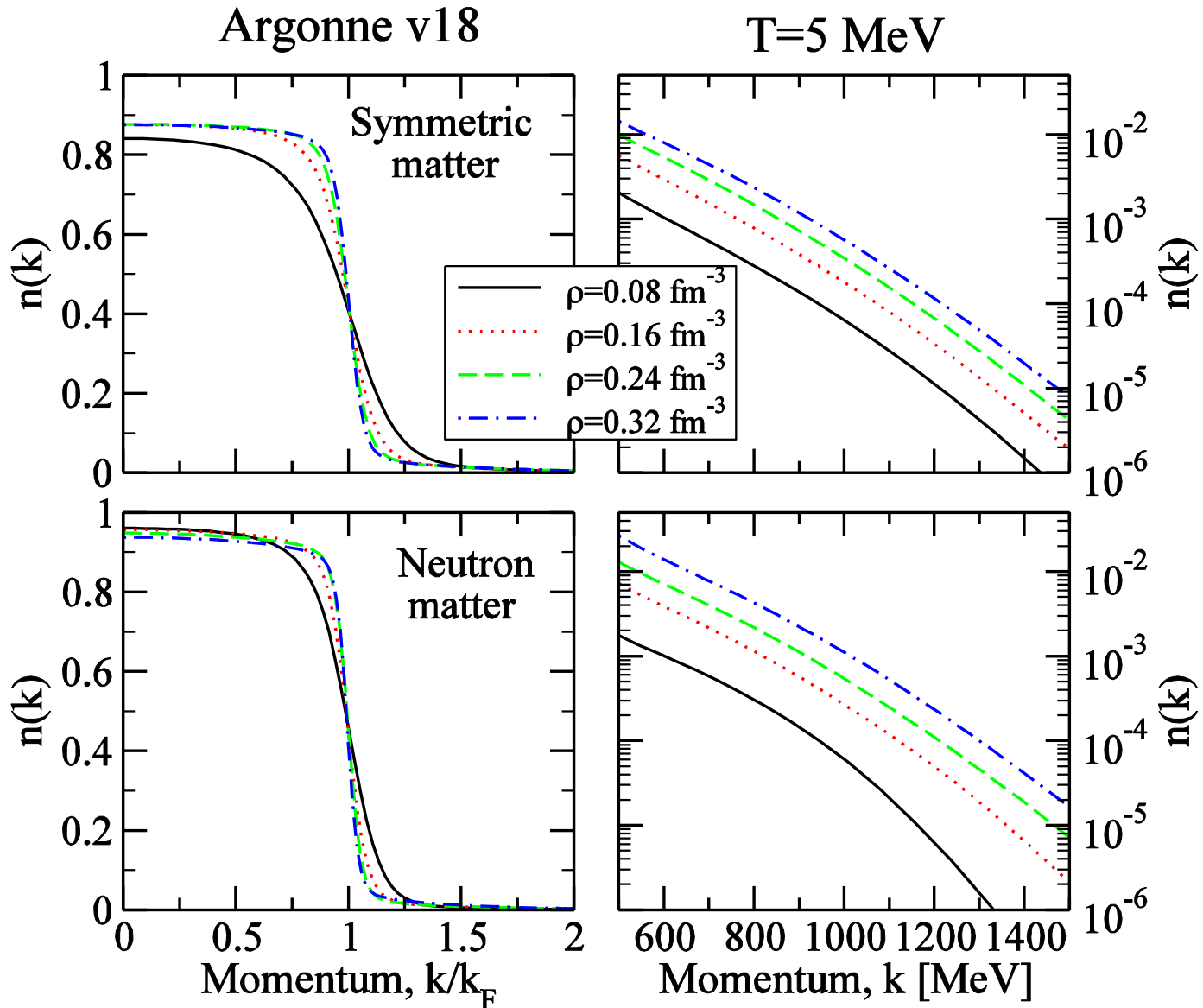
The less abundant component (the protons) are very much affected by thermal effects.

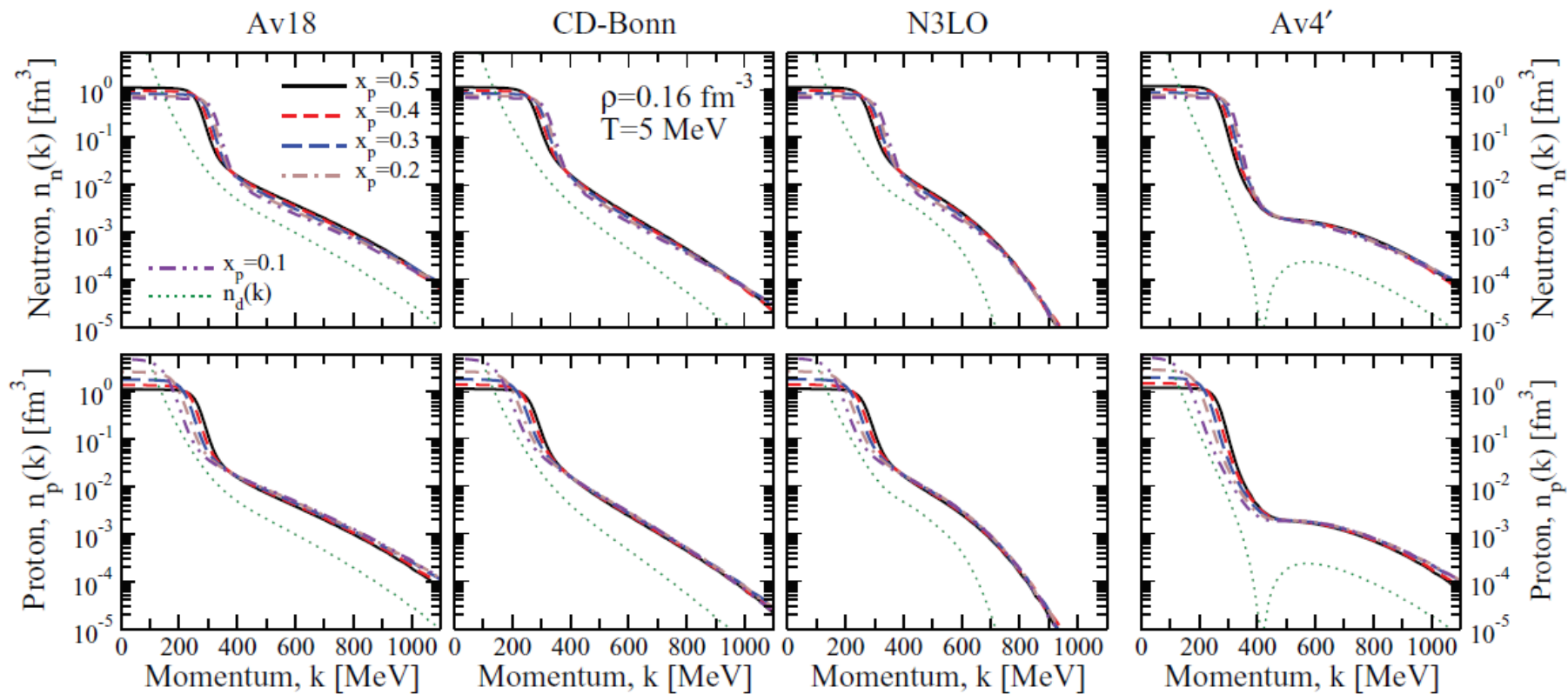
$$\rho = 0.16 \text{ fm}^{-3} \text{ and } T = 5 \text{ MeV}$$



Momentum distributions of symmetric and neutron matter at $T=5$ MeV

High-momentum tails increase with density (Short-range correlations)



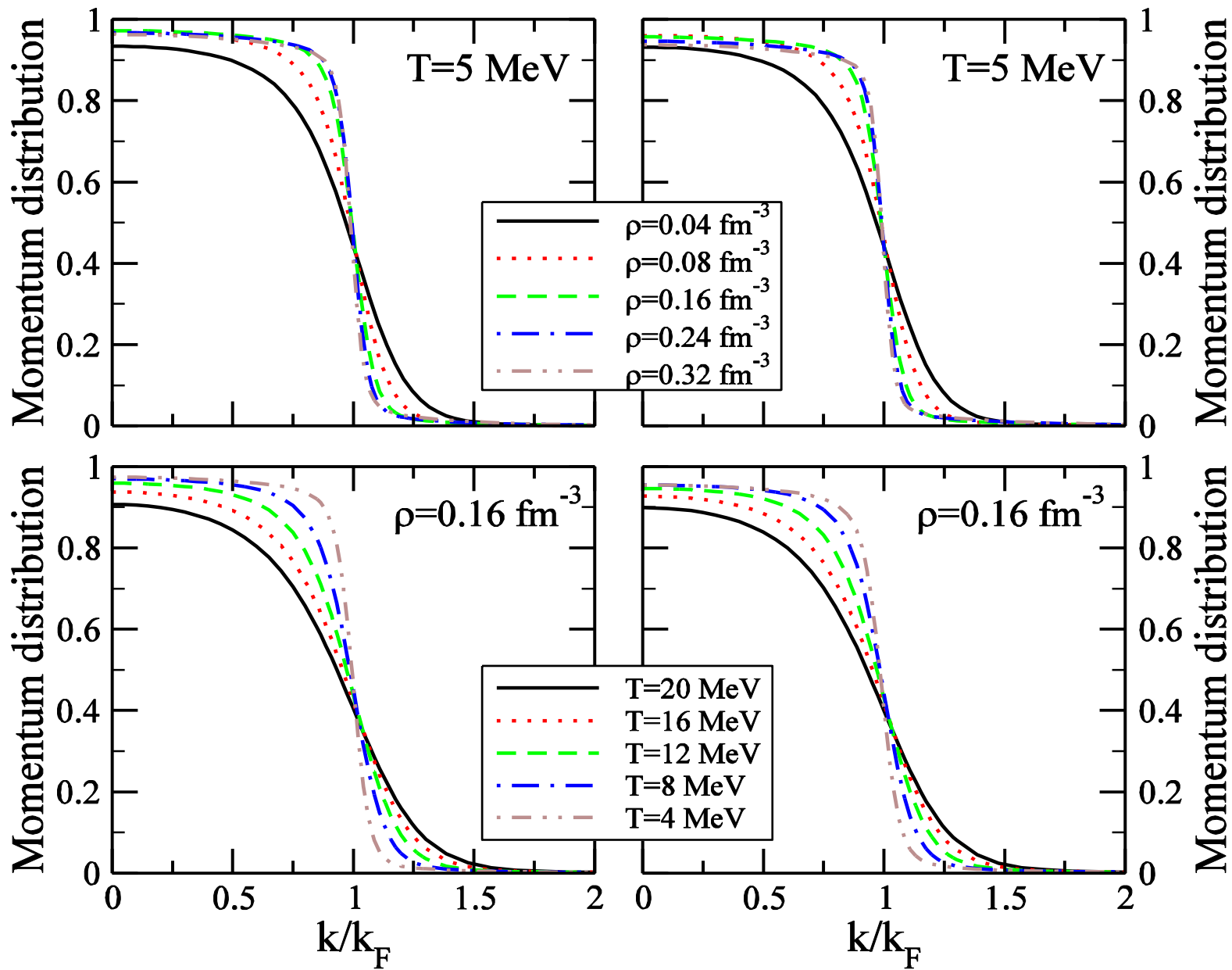


High-momentum components change very little with isospin.
 This suggests that, when the momentum distribution is normalized to unity, high-momentum components are basically determined by the total density of the system.

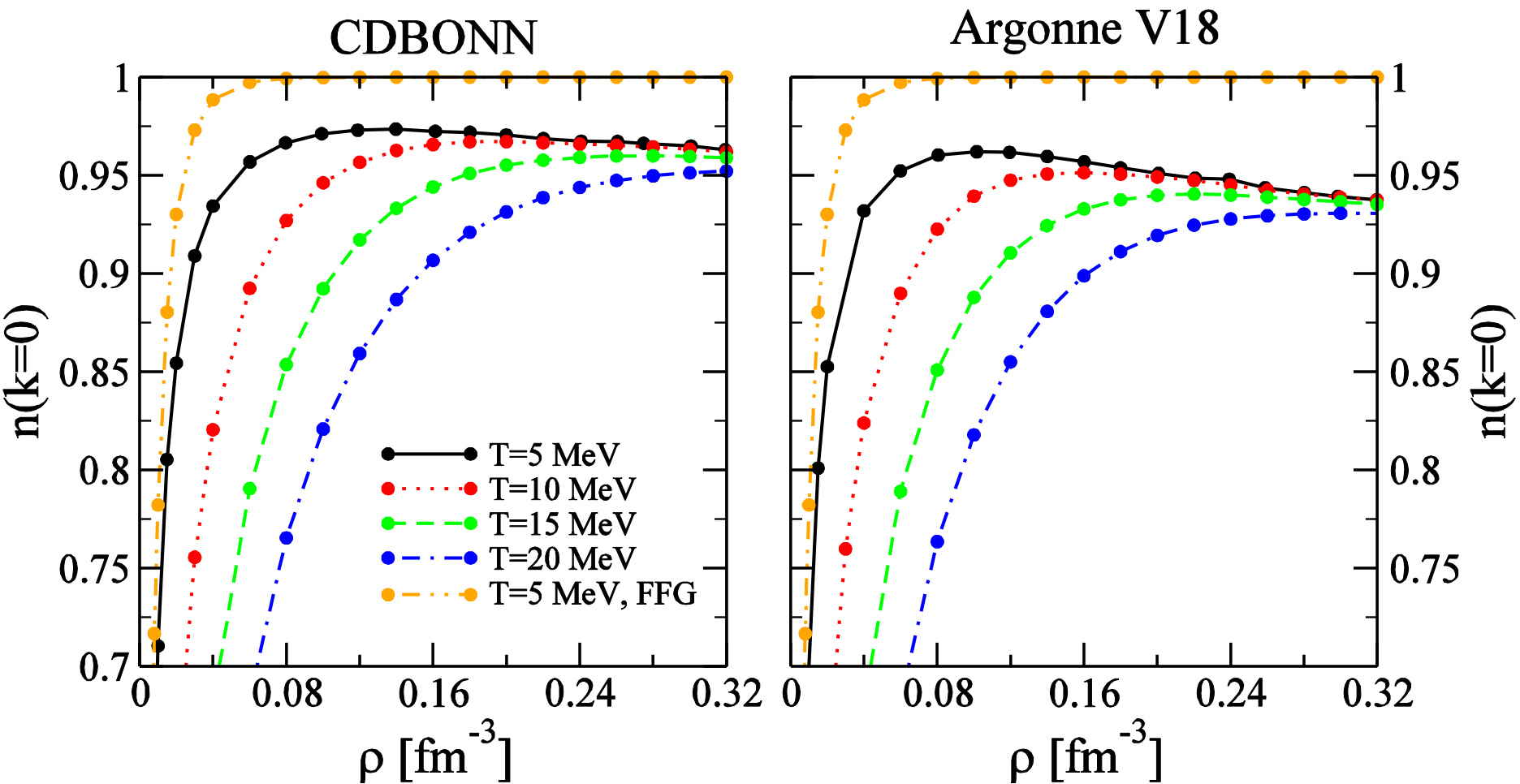
$n(k)$ for neutron matter

CDBONN

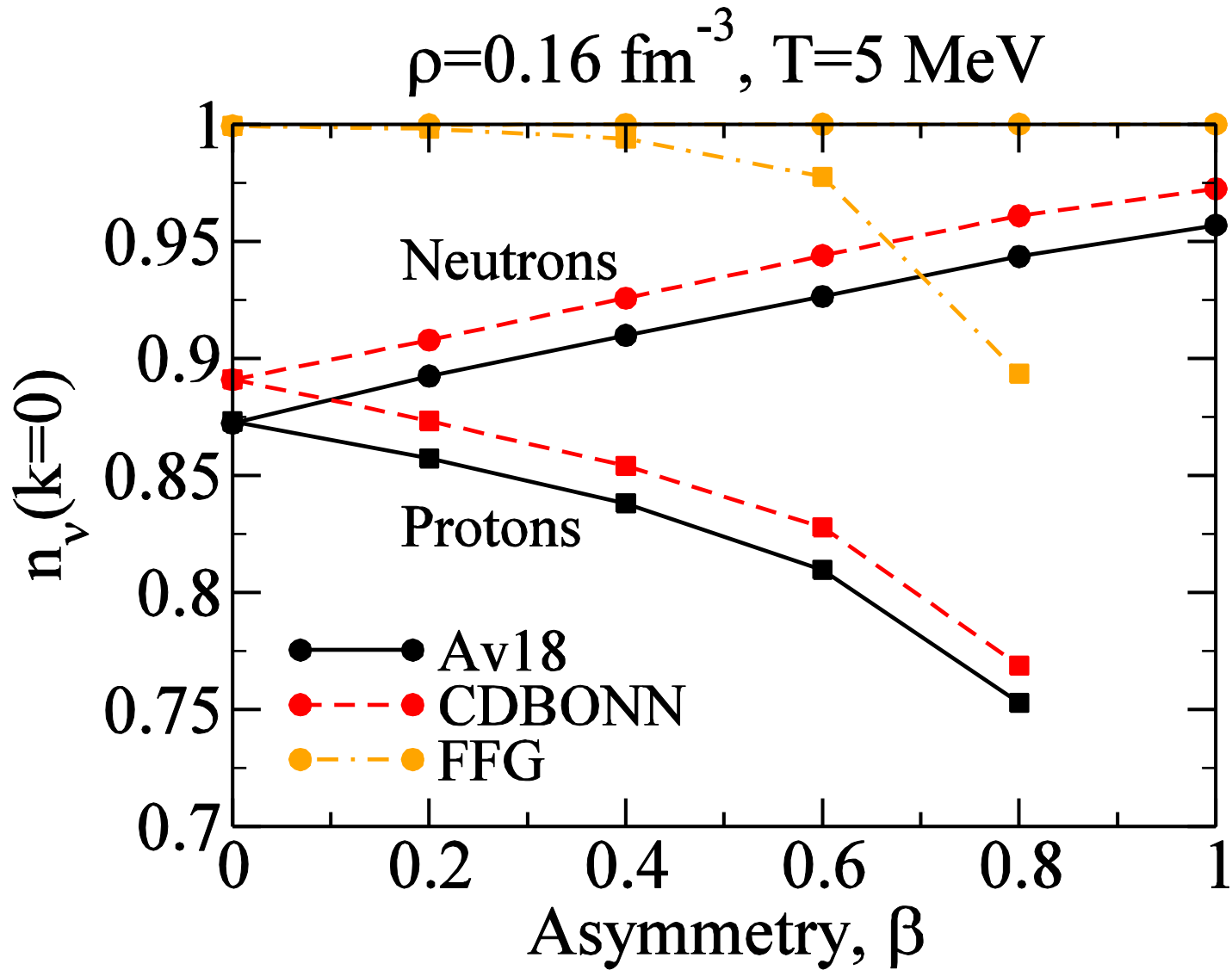
Argonne V18

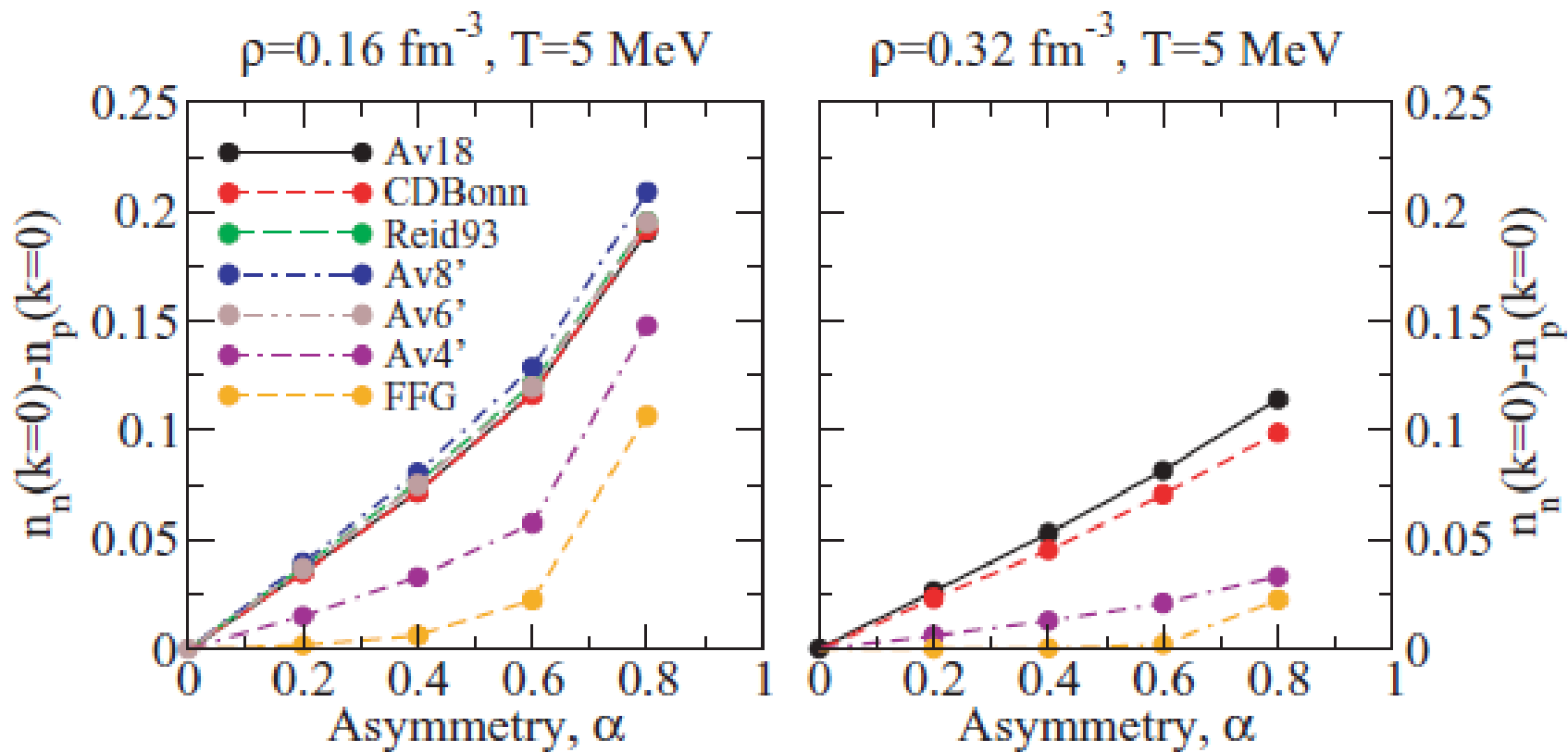


Occupation of the lowest momentum state as a function of density for neutron matter.



Dependence of $n(k=0)$ on the asymmetry





$n(k=0)$ for nuclear and neutron matter,

$$\rho = 0.16 \text{ fm}^{-3} \text{ and } T = 5 \text{ MeV}$$

Interaction	Symmetric	Neutron
CDBONN	0.891	0.972
Reid93	0.872	0.962
Argonne v18	0.872	0.957
Argonne v8'	0.863	0.956
Argonne v6'	0.879	0.964
Argonne v4'	0.946	0.971
FFG	0.9993	0.999991

Neutron matter is systematically less depleted

		SNM			PNM		
	k_i k_f	ϕ_2	K/A	E/A	ϕ_2	K/A	E/A
CDB	0 k_F	0.762	15.8	-12.6	0.869	28.9	10.1
	k_F $2k_F$	0.211	12.0	-1.54	0.121	9.87	3.78
	$2k_F$ ∞	0.027	6.95	-0.59	0.010	3.78	0.28
	0 ∞	1.00	34.7	-14.7	1.00	42.5	14.1
Av18	0 k_F	0.755	15.6	-7.65	0.863	28.7	11.6
	k_F $2k_F$	0.194	11.4	-0.997	0.119	10.3	3.24
	$2k_F$ ∞	0.051	14.5	-1.29	0.018	7.16	0.32
	0 ∞	1.00	41.5	-9.94	1.00	46.2	15.2
FFG	0 k_F	0.861	17.7	17.7	0.912	30.4	30.4
	k_F $2k_F$	0.139	6.00	6.00	0.089	5.75	5.75
	$2k_F$ ∞	0.00	0.00	0.00	0.00	0.00	0.00
	0 ∞	1.00	23.7	23.7	1.00	36.2	36.2

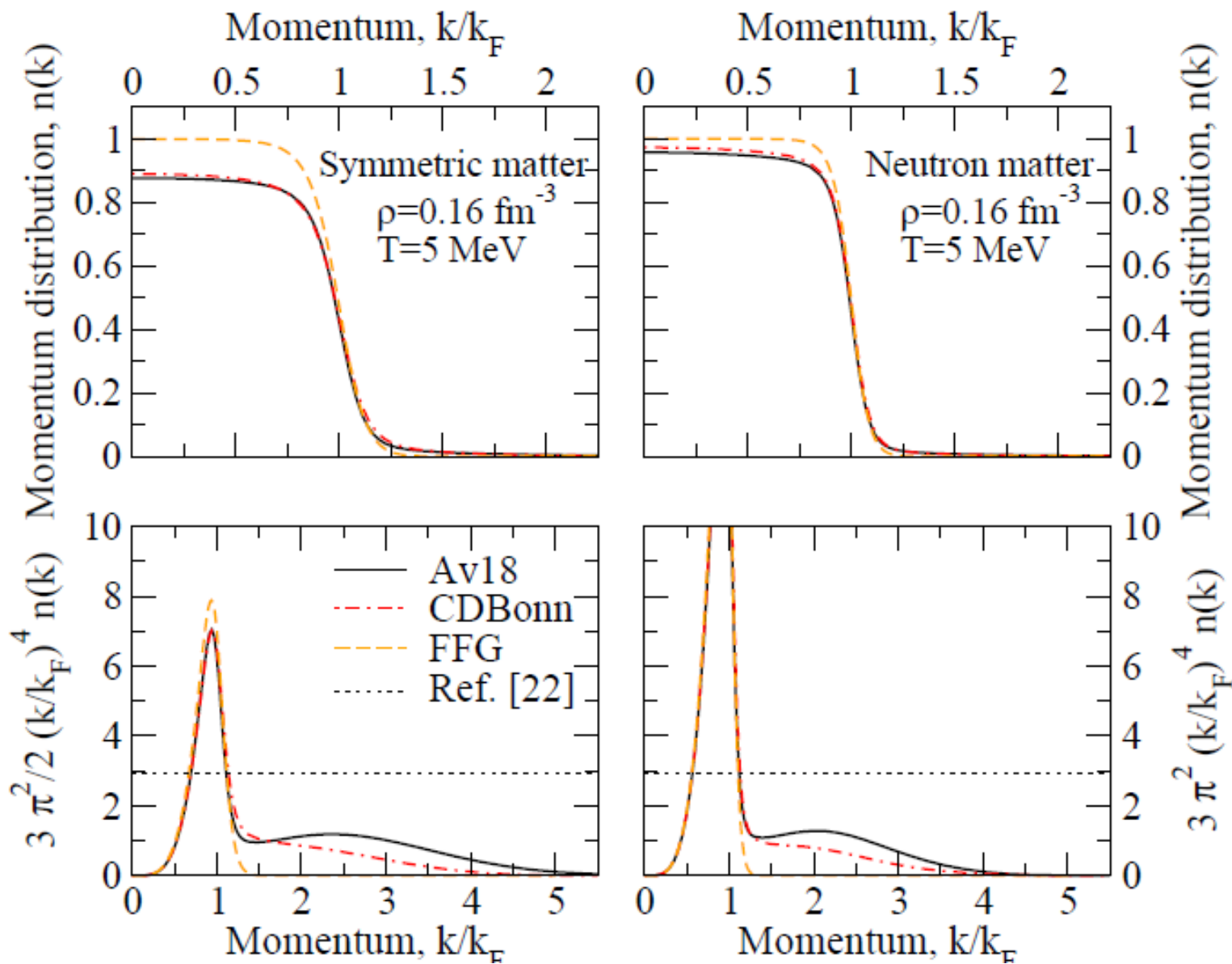
Contributions of different momentum regions to the total density (columns 3 and 6) , kinetic (4 and 7, in MeV) and total energies (5 and 8, in MeV) for SNM (columns 3,4 and 5) and PNM (columns 6,7 and 8) with different NN interactions.

The FFG case is also included. All results are computed at $\rho=0.16 \text{ fm}^{-3}$ and $T=5 \text{ MeV}$

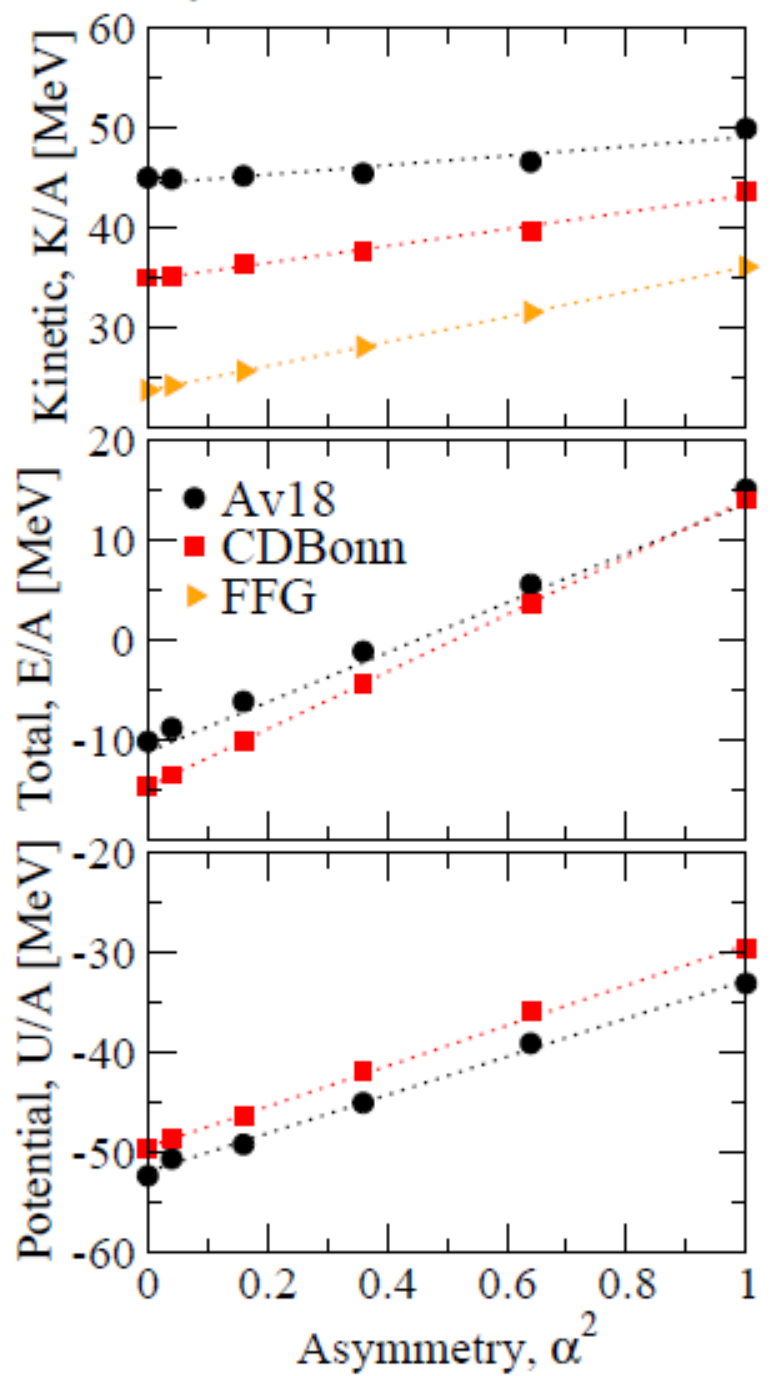
Integrated strength over different regions

$$\phi_m(k_i, k_f) = \frac{\nu}{2\pi^2\rho} \int_{k_i}^{k_f} dk k^m n(k)$$

Importance of the high momentum components



$\rho=0.16 \text{ fm}^{-3}$, $T=5 \text{ MeV}$



Isospin asymmetry dependence of the kinetic and potential energy contributions to the total energy. For the CDBonn (squares) and Av18 (circles) potentials. The triangles of the upper panel give the energy of the FFG in the same conditions, $\rho= 0.16 \text{ fm}^{-3}$ and $T=5 \text{ MeV}$.

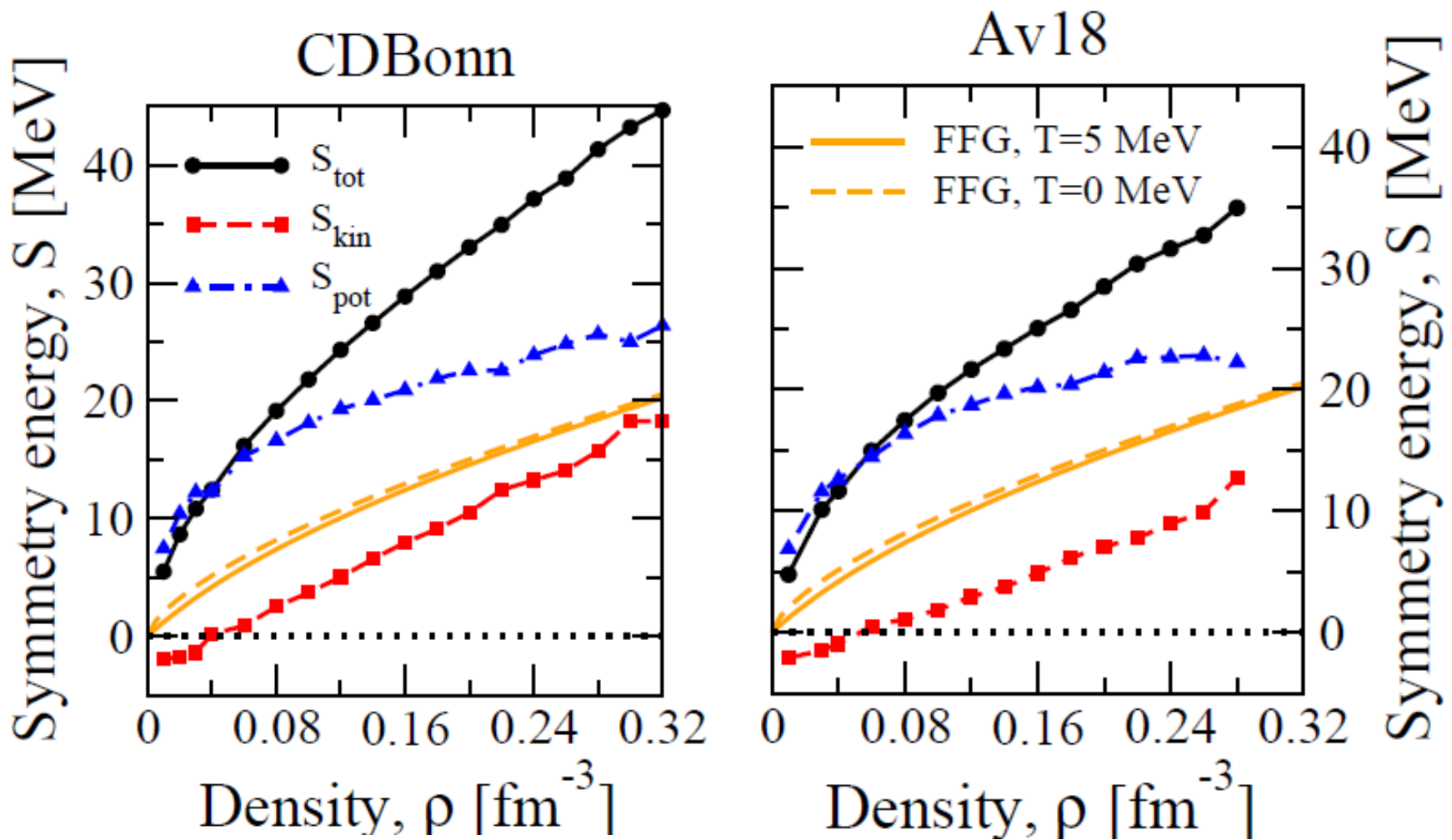
Almost linear dependence \implies quadratic dependence on the asymmetry parameter. Different slopes.

	S_{tot}	S_{kin}	S_{pot}	L
Av18	25.1	4.9	20.2	37.7
Nij1	27.4	4.6	22.8	48.5
CDBonn	28.8	7.9	20.9	52.6
N3LO	29.7	7.2	22.4	55.2

Total, kinetic and potential contributions in MeV to the symmetry energy. At $\rho = 0.16 \text{ fm}^{-3}$ and $T = 5 \text{ MeV}$ for different NN interactions.

The difference in total kinetic energy of PNM and SNM is smaller for the correlated case than for the FFG

The symmetry energy is dominated by the potential energy



Components of the symmetry energy for the CDBonn and Av18 potentials at $T=5$ MeV. The continuous (dashed) lines correspond to the FFG symmetry energy at $T=5$ ($T=0$) MeV. NO THREE-BODY FORCE.

Summary

- ❖ At the same density, neutron matter is less correlated than nuclear matter, in the sense that $n(k)$ is less depleted. The variation of kinetic energy respect to the FFG is smaller for neutron matter than for nuclear matter.
- ❖ The kinetic symmetry energy is very small (compared with the FFG) and could be even negative. The potential part of the symmetry energy is very large. The main contribution coming from the tensor part of the NN interaction and the partial waves where the tensor is acting.
- ❖ The kinetic and the potential energy have a quadratic dependence on the asymmetry parameter.

The BHF values for the symmetry energy and L (calculated with the Av18 and a Urbana IX three-body force) are compatible with the experimental determinations.

- ❖ Important interplay between thermal and dynamical correlation effects. For a given temperature and decreasing density, the system approaches the classical limit and the depletion of $n(k)$ increases. Not to confuse with correlation effects.
- ❖ Three-body forces should not change the qualitative behavior of $n(k)$.

Present and future work (uniform infinite systems)

Three-body forces. How should be incorporated?

Present strategy for uniform systems: Average the interaction over one particle to get a density dependent two-body force.

One should do that very carefully to respect the antisymmetry. Also necessary: Perform a three-hole line calculation with the explicit use of three-body forces.

Response functions of neutron and nuclear matter.

The depletion and spreading of the strength of the single particle states should be reflected in the quenching and spreading of the response. Already at the level of the dressed Lindhard function.

Work out the two-body correlations (distribution functions) from the two-body propagator. That it is also necessary for the average of the three-body forces.

Go beyond ladder approximation. To include long-range correlations. RPA with dressed ph-propagators.

Pairing!

Applications to nuclear star physics. Beta-stable matter. Hyperons.

Special thanks to the people interested in these subjects for enlightening discussions and collaborations!

Wim Dickhoff (St. Louis)

Herbert Muether (Tubingen)

Arnau Rios (Surrey)

Carlo Barbieri (Surrey)

Arianna Carbone (Darmstadt). See her thesis for three-body forces

Isaac Vidaña (Coimbra)

D. Ding (PhD student at Washington University in St. Louis)

